JOURNAL OF GEOPHYSICAL RESEARCH, VOL. 103, NO. B5, PAGES 9807–9825, MAY 10, 1998

Graben formation associated with recent dike intrusions and volcanic eruptions on the mid-ocean ridge

William W. Chadwick Jr.

Cooperative Institute for Marine Resources Studies, Oregon State University, Hatfield Marine Science Center Newport

Robert W. Embley

Pacific Marine Environmental Laboratory, NOAA, Hatfield Marine Science Center, Newport, Oregon

Abstract. Grabens have been mapped immediately adjacent to recently erupted submarine lava flows on the Cleft and CoAxial segments of the Juan de Fuca Ridge (JdFR). The grabens are 10–100 m wide and 5–15 m deep and are located uprift and/or downrift of the eruptive vents that fed the flows. We interpret that these structures formed (or were reactivated) directly over the dike that fed the eruptions as it was intruding toward the surface. These graben structures are primary conduits for diffuse hydrothermal venting on the seafloor during the cooling of newly intruded dikes. The axial summit "graben" or "caldera" on the East Pacific Rise (EPR) in some locations has similar dimensions to the grabens observed on the JdFR, and we interpret that it too may be a dike-induced graben structure (although often buried by subsequent eruptions where it is narrowest). These grabens on the JdFR and the EPR are distinctly narrower and deeper than grabens that formed during well-documented dike intrusions on slow spreading rifts on land (Iceland and Afar). Mechanical modeling suggests that narrow grabens would form when a dike is at shallow depth where it imposes a high stress perturbation on the ambient stress state to cause faulting. Therefore the narrow grabens on the JdFR and EPR imply that a relatively high level of horizontal compressive stress typically exists perpendicular to the ridges, and this must be overcome by high dike-induced perturbations to cause faulting. This is probably because gradual plate spreading rarely gets enough time to lower the compressive stress significantly due to the high frequency of dike intrusion events relative to the plate spreading rate. The dikes that do intrude in this environment must have relatively high internal magma pressure. Therefore the size and character of dike-induced grabens that form at the surface on intermediate to fast spreading ridges reflect the fact that volcanism dominates over tectonism in regulating the local stress state where a robust magma supply is available.

1. Introduction

Dikes are the most common near-surface conduits for magma within volcanic rift zones. Dike emplacement induces stress in the surrounding rock which generates seismicity and deformation, frequently including the formation of a graben at the surface. The size, distribution, and orientation of such grabens can be interpreted in terms of the theoretical stress states associated with dike intrusion [*Pollard et al.*, 1983; *Mastin and Pollard*, 1988; *Rubin and Pollard*, 1988; *Rubin*, 1992].

Surface faulting and graben formation have been observed during dike intrusions on land, but this relationship has not been well documented in volcanic rift zones on the mid-ocean ridge (MOR). In fact, much about the dynamics of volcanic events on the MOR is still largely unknown, because the events are difficult to observe and monitor. On the basis of theoretical modeling and the similarity of dike-induced graben formation in diverse settings on land, one might expect to see similar behavior on the MOR [*Davis*, 1984; *Head et al.*, 1996]. However, some aspects of the MOR tectonic environment are unique (the thin oceanic crust and the wide range of spreading rates, for example) and could have an effect on the character of dike emplacement and the resulting surface deformation [*Curewitz and Karson*, 1997].

Recent seafloor eruptions on the Juan de Fuca Ridge (JdFR) have provided the opportunity for detailed mapping of geologic structures near eruption sites. We present here the results of this geologic mapping, compare seafloor structures to those observed on land, and explore the implications of these structures in terms of previous modeling results and observations at other mid-ocean ridges.

Throughout this paper we use the terms "fissure," "fault," and "graben" based on the following standard definitions [*Park*, 1983]. Fractures whose walls have moved apart by pure extension are called fissures. Where there is shear across the fracture plane (measurable displacement of one side relative to the other in the plane of the fracture), the fracture is termed a fault. A graben is a descriptive term referring to a linear topographic depression due to subsidence along inward facing normal faults.

Paper number 97JB02485.
0148-0227/98/97JB-02485$09.00

2. How Dike Intrusions Cause Graben Formation

The intimate connection between dike intrusion and faulting/fissuring at the surface has been documented by field observations and geodetic monitoring in volcanic rift zones (Figure 1a). Grabens have formed or have been reactivated over dike intrusions at active volcanoes in a variety of tectonic settings, including Kilauea, Hawaii [*Richter et al.*, 1964; *Richter et al.*, 1970; *Jackson et al.*, 1975; *Moore et al.*, 1980; *Pollard et al.*, 1983; *Wolfe et al.*, 1988]; Etna, Italy [*Murray and Pullen*, 1984]; Laki and Krafla, Iceland [*Thorarinsson*, 1969; *Björnsson et al.*, 1979; *Sigurdsson*, 1980]; and the Asal-Ghoubbet rift, Djibouti (Afar) [*Abdallah et al.*, 1979; *Ruegg et al.*, 1979; *Tarantola et al.*, 1979; *Stein et al.*, 1991]. Graben subsidence can range from a few centimeters up to a few meters, and graben widths can vary from a few meters to several kilometers. Detailed seismic and geodetic monitoring has demonstrated that it is the intrusion of the dike that triggers the surface faulting and not vice versa [*Rubin and Pollard*, 1988; *Rubin*, 1992]. During a dike intrusion in 1977 at Krafla, for example, surface deformation propagated downrift at about the same rate as an earthquake swarm that accompanied the leading edge of the dike, which was unequivocally located when it intersected a geothermal borehole and erupted a small amount of tephra at the surface [*Brandsdottir and Einarsson*, 1979; *Larsen et al.*, 1979; *Hauksson*, 1983; *Rubin*, 1992]. Grabens do not always form above an intruding dike, but if one does form, this always occurs before the dike reaches the surface. If an eruption follows later, the eruptive fissure would open within the floor of the newly subsided graben.

These field observations were later explained and interpreted by theoretical and physical modeling of the mechanical consequences of dike intrusion [*Pollard et al.*, 1983; *Mastin and Pollard*, 1988; *Rubin and Pollard*, 1988; *Rubin*, 1992]. In addition, the models allow various parameters of a subsurface dike to be quantified if enough geodetic data are available. *Pollard et al.* [1983] showed that when a dike has not yet reached the Earth's surface, its internal pressure compresses the surrounding rock and produces horizontal elastic displacements directed away from the dike. At the surface, these displacements are greatest at some distance away from the plane of the dike, because the dike top is still at some depth and a point at the surface directly above the dike experiences little or no displacement (Figure 1b). As a consequence, two zones of maximum horizontal tension are created at the surface on either side of the dike plane, between the static area above the dike and the areas to either side which are being displaced outward (Figure 1c). This is what leads to graben formation above a dike: these two zones of maximum horizontal tension and extensional strain often produce two parallel zones of fissuring and normal faulting (inelastic deformation) at the surface (Figure 2).

The modeling also shows that these effects vary as a function of the dike depth. The distance between the two high strain zones decreases as the dike nears the surface (Figure 3), and this distance is approximately equal to twice the depth to the top of the dike [*Pollard et al.*, 1983; *Mastin and Pollard*, 1988]. This means that as the dike intrudes upward, the two high strain zones at the surface actually move inward toward the dike plane (Figure 4). This occurs because the area above the dike that does not "feel" the horizontal compression exerted by the dike walls becomes smaller and narrower as the dike nears the surface. Thus the width of a graben that forms during an

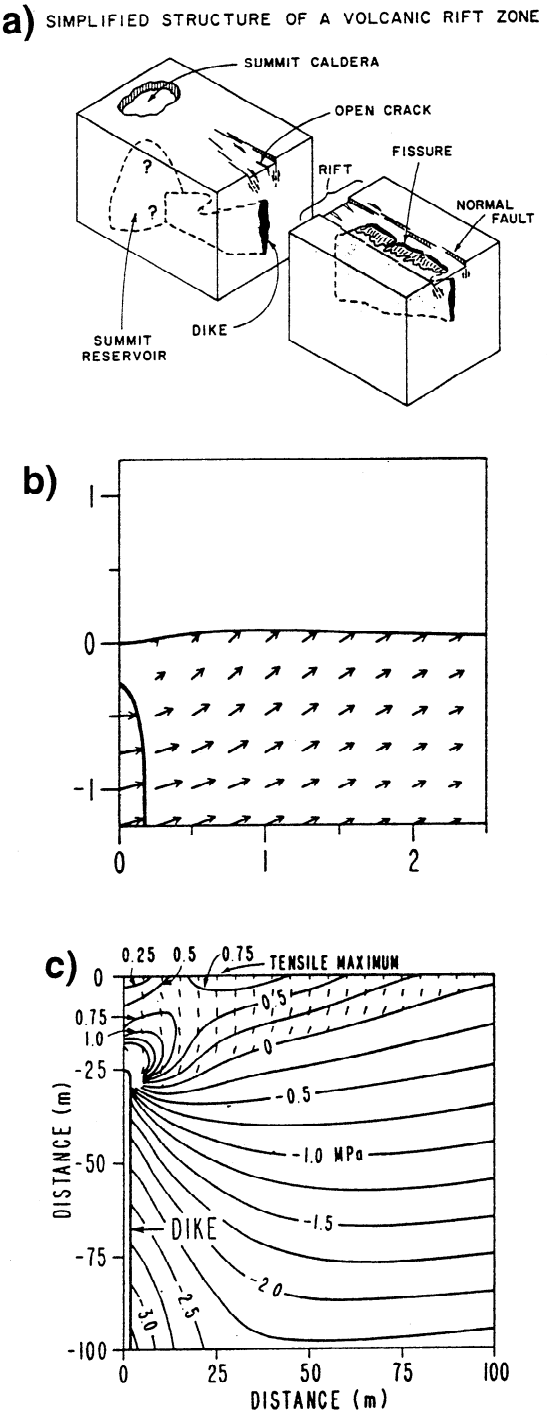

Figure 1. (a) Schematic drawing of grabens forming over an intruding dike in a volcanic rift zone. (b) Displacement vectors from a model in which a dike in a semi-infinite medium is subject to internal pressure. Note that surface displacements are near zero directly over the dike and reach a maximum at some distance outward from the dike plane. This creates tension between these areas. (c) Contours of the maximum principal stress near a model dike (compression is negative; tension is positive). Within the zone of near-surface tension, short dashed lines are trajectories of the minimum principal stress and indicate potential planes of secondary cracking or faulting. Note that the tensile maximum at the surface is located at a distance from the dike plane about equal to the depth to the dike top. This is the most likely location for fissure/graben formation. All figures are from *Pollard et al.* [1983].

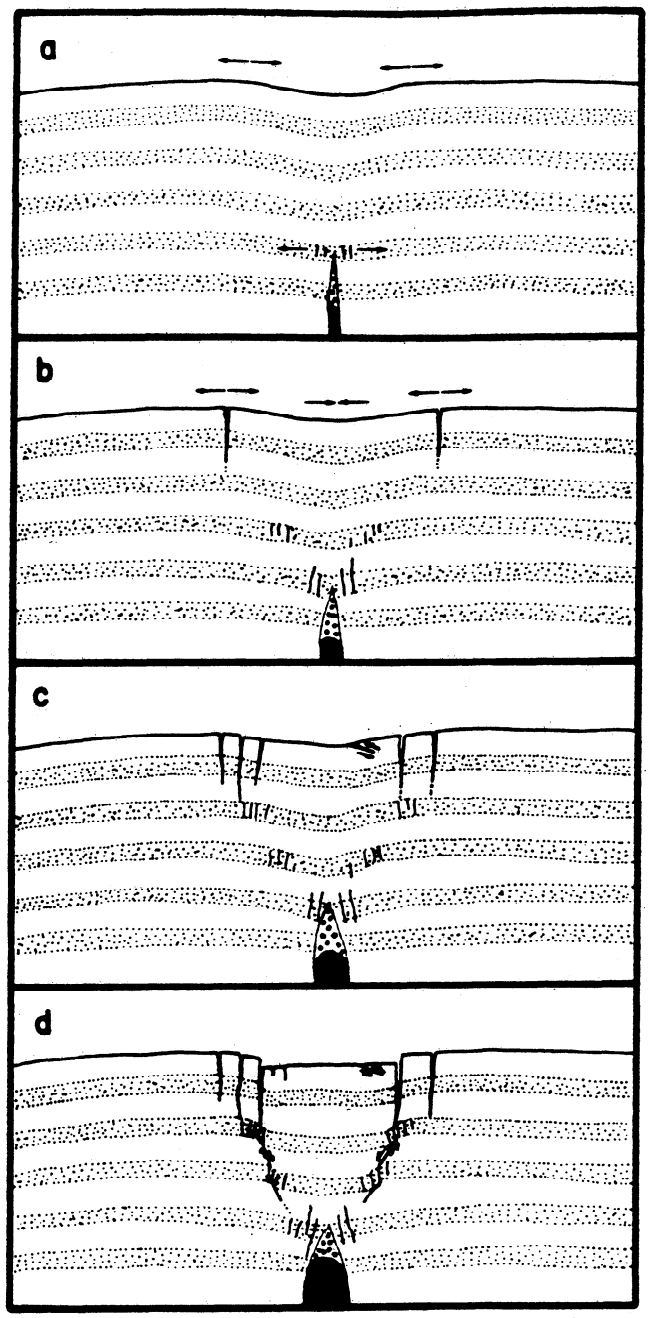

Figure 2. Generalized sequence of fault and fissure growth above a shallow dike leading to graben formation, based on results of physical model experiments in the laboratory. From *Mastin and Pollard* [1988].

intrusion can give an estimate of the depth of the dike beneath it (at the time the faulting occurred).

Another key modeling result is that the magnitude of the maximum horizontal extensional strain at the surface dramatically increases as the dike nears the surface [*Pollard et al.*, 1983; *Mastin and Pollard*, 1988]. In other words, at the same time that the distance between the high strain zones is decreasing, the magnitude of that strain is increasing (Figure 3). An implication of this result is that the width of a graben is an indirect measure of the preexisting ambient stress state; since graben width is related to dike depth, it also reflects the magnitude of the dike-induced perturbation to the near-surface stress field that was required to initiate faulting. For example, an area "primed" for extensional faulting would fail with only a small perturbation from a dike, which would occur when the dike was deep, and so the graben formed would be wide (Figure 4a). On the other hand, if the area was not as primed to fail, then it would take a larger perturbation from a dike to cause surface faulting, which would occur when the dike was shallow, and so the graben produced would be narrow (Figure 4b). Any graben faulting that might occur must take place before a dike reaches the surface because once this happens, the entire stress field changes to compression [*Pollard et al.*, 1983].

The width of a dike can be estimated by measuring the amount of horizontal extension accommodated by faulting at the surface. *Mastin and Pollard* [1988] found that in their physical models the amount of surface extension associated with graben formation was roughly 2/3 the dike width. This result is a useful guide, although *Rubin* [1992] showed that in elastic numerical experiments the dike width to extension relationship also depended somewhat on the model boundary conditions.

3. Observations of Dike-Induced Grabens on the Juan de Fuca Ridge

Recent seafloor eruptions have been documented on two segments of the Juan de Fuca Ridge (JdFR): the Cleft and CoAxial segments (Figure 5). The Cleft eruption occurred between 1983–1987 and was discovered by a combination of hydrothermal plume surveys [*Baker et al.*, 1987, 1989], seafloor geologic mapping [*Embley et al.*, 1991; *Chadwick and Embley*, 1994; *Embley and Chadwick*, 1994], and repeated bathymetric mapping with multibeam sonar [*Chadwick et al.*, 1991; *Fox et al.*, 1992]. The CoAxial eruption occurred in June–July 1993 during a seismic swarm that was detected as T waves by U.S. Navy hydrophones [*Dziak et al.*, 1995; *Fox et al.*, 1995]. Before the swarm had ended, active hydrothermal plumes and a newly erupted lava flow were discovered [*Baker et al.*, 1995; *Embley et al.*, 1995b]. Detailed geologic mapping at both the Cleft and CoAxial eruption sites have revealed well-defined grabens

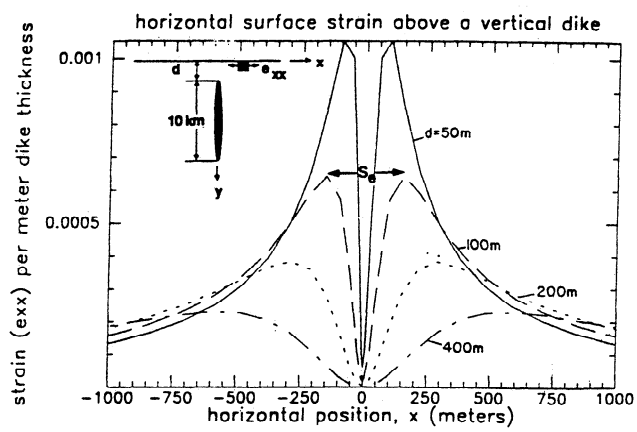

Figure 3. Horizontal extensional strain parallel to the Earth's surface per meter of dike thickness versus horizontal position measured from the point immediately above the dike, in a direction perpendicular to the dike plane. Curves are for different dike depths: $d = 50$ m (solid), 100 m (long-dashed), 200 m (short-dashed), and 400 m (long-dashed, short-dashed). Note that the strain maxima move inward toward the dike plane and increase in magnitude as the depth to the dike top decreases. From *Mastin and Pollard* [1988].

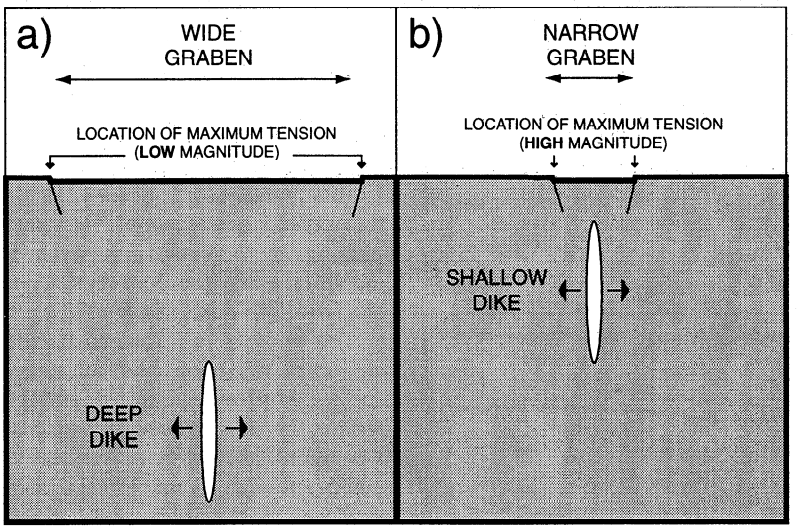

Figure 4. Cartoon showing the relationships between dike depth, graben width, magnitude of dike-induced stress perturbation, and location of zones of maximum tension at the surface which are the most likely areas for fissure/graben formation, if it occurs. An individual dike may (a) start deep and (b) migrate upward. A dike will always impose elastic strains at the surface, whereas inelastic deformation (faulting) will only occur sometimes. Faulting will occur if and when the ambient stress plus the dike-induced stress perturbation exceeds the tensional strength of the rock. Therefore the width of a graben that forms during a dike intrusion tells something about the magnitude of the ambient stress, because the dike-induced stress varies in magnitude and location with dike depth (see text for discussion).

associated with the recent eruptive vents. In some cases, the grabens appear to be new features that formed during the eruption, and in others the grabens appear to have formed earlier but were reactivated during the most recent events. In the former cases, there is no conclusive proof that the grabens formed at the same time as the eruptions (this could only come from geodetic monitoring or detailed preeruption and post-eruption site surveys), but several lines of evidence support this interpretation.

3.1. Geologic Mapping Methods

The geologic mapping presented below is based on seafloor photographs, video, and microbathymetry from camera tows, as well as observations from the remotely operated vehicle ROPOS and the submersible *Alvin*, all acoustically navigated with long-baseline transponders. In addition, high-resolution bathymetric surveys of selected areas hundreds of meters on a side have been collected with a Mesotech sonar. The Mesotech is a 675 kHz, "pencil beam" scanning sonar with a depth resolution of ~0.1 m when mounted on *Alvin*. The sonar head repeatedly sweeps from side to side, and as *Alvin* drives forward (typically at ~20 m altitude), it collects a zigzag pattern of soundings on the seafloor. These sweeps can be displayed as a series of individual depth profiles or they can be merged with the subnavigation and then gridded to make a bathymetric map [*Chadwick and Embley*, 1995]. The Mesotech data have been especially valuable in mapping structures that are too small to be resolved by surface-based multibeam sonar but are larger than the limited scale of submersible or camera observations. Another important data set is AMS-60 side-scan sonar imagery of selected areas, collected in 1996 from the NOAA ship *Discoverer* [*Chadwick et al.*, 1996]. The AMS-60 tow fish is towed at ~1.5 knots, 150–200 m above the seafloor (for a 2-km-wide swath), and sends out acoustic pulses at 60 kHz from each side of the tow fish. The amplitude and phase of reflected acoustic energy are then recorded and processed to produce images of the seafloor with a pixel resolution of 1–2 m, which are particularly useful for highlighting seafloor texture and structures.

3.2. CoAxial Segment Eruption

The 1993 T wave swarm at CoAxial migrated 60 km northward along the ridge segment over the first 3 days, which was interpreted as evidence for lateral propagation of a dike [*Dziak et al.*, 1995]. The swarm then localized for the next 2 weeks near 46°31'N where a new lava flow was later found, an area later named the "Flow site." The 1993 dike initially "overshot" the Flow site and apparently intruded ~10 km farther north, based on the extent of located earthquakes [*Dziak et al.*, 1995]. The entire T wave swarm consisted of 676 earthquakes, most of them well below M3 [*Dziak et al.*, 1995], indicative of shallow faulting events during the intrusion. The main 1993 lava flow is the product of a fissure eruption where the dike breached the surface and is 2.5 km long, is 300 m wide, and has a maximum thickness of over 30 m [*Chadwick et al.*, 1995; *Embley et al.*, 1995b]. The areas immediately north and south of the 1993 flow have been mapped in detail, revealing that grabens, which are centered on the eruptive axis of the flow, underlie it both uprift and downrift (Figure 5b).

The graben just north of the main 1993 flow is 10–20 m wide and 5–15 m deep and extends northward for at least 200 m (Plates 1 and 2a–2c). A small amount of 1993 lava erupted out of this graben and slightly overflowed it ~100 m north of the main flow (Plates 1 and 2c). Mesotech profiles from north to south along the axis of the graben (Plates 1c and 1d) show it gradually being filled, first by the small satellite flow and then by the main 1993 flow. Several other small flows have also been mapped farther to the north along strike [*Spiess and Hildebrand*,

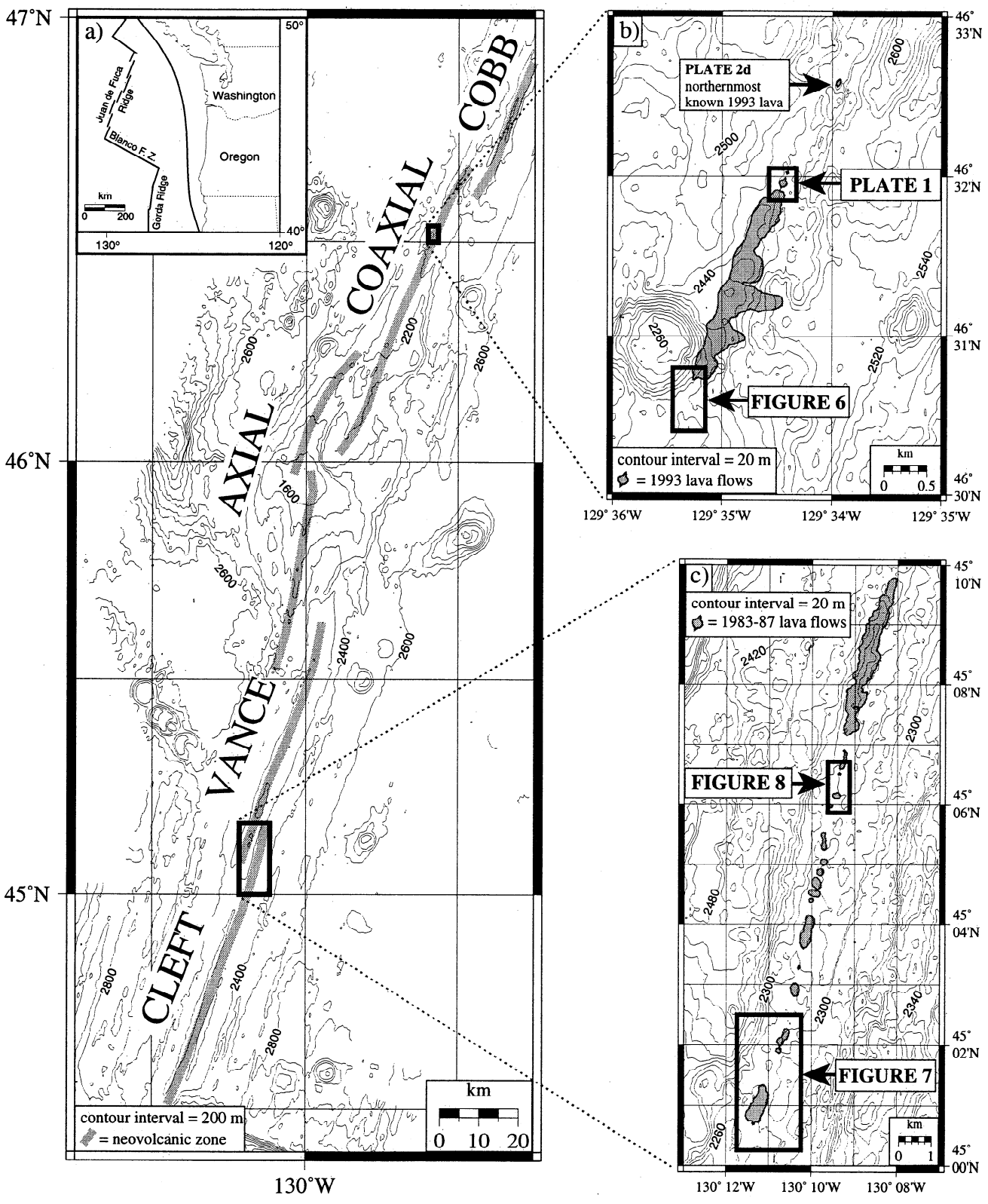

Figure 5. Location maps of (a) Juan de Fuca Ridge (segment names are labeled adjacent to the neovolcanic zone which is stippled), (b) CoAxial Flow site, and (c) North Cleft site, showing the locations of Plates 1 and 2d and Figures 6, 7, and 8. Lava flows associated with recent eruptions are stippled.

1993]. One of these small flows of 1993 lava was found 1.5 km north of the main flow (Figure 5b and Plate 2d) during *Alvin* dive 2794 and was also confined within a graben that is 20 m wide and 2 m deep (M. R. Perfit, personal communication, 1996). The side-scan imagery shows that these two grabens north of the 1993 flow are connected along strike by a system of discontinuous grabens and fissures, probably along the path of the CoAxial dike. In both cases, the graben walls appeared to

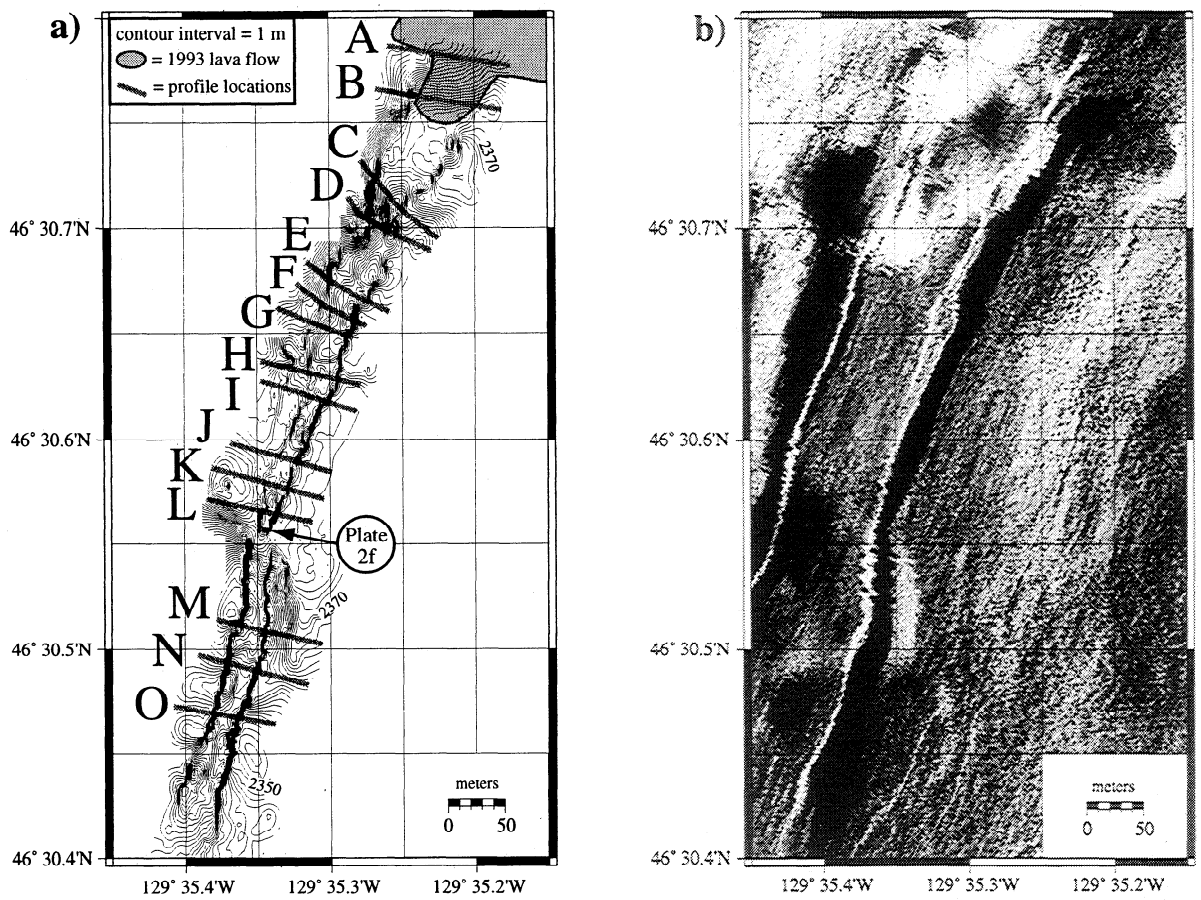

Figure 6. Mesotech and side-scan sonar data from the CoAxial Flow site showing the graben at the southern end of the main 1993 CoAxial lava flow (location is shown in Figure 5b). (a) Mesotech sonar bathymetry (1-m contours) from *Alvin* dives 2671 and 2994. Lettered lines (A-O) show locations of individual Mesotech depth files in Figures 6c and 6d. Light gray stipple shows southern end of 1993 lava flow. (b) AMS-60 side-scan sonar image (illuminated from SE; white is high reflectivity, black is acoustic shadow). Lower slope of Cage Volcano is in the upper left. (c) and (d) Individual Mesotech depth profiles (locations are shown in Figure 6a) offset from one another by an arbitrary depth for clarity.

be freshly broken (Plate 2e) and the erupted lava confined within the grabens is clear evidence that the 1993 dike underlies the grabens at shallow depth. We interpret that these grabens formed directly above the dike as it was intruding, just before it reached the surface. This relative timing is confirmed by the observation that the 1993 lavas are not faulted where they bury the graben faults (Plate 2c). The width of the two grabens implies that the top of the dike was only at 5–10 m depth when they formed, and that the top of the dike is very shallow for several km north of the main eruption site.

South of the main 1993 flow, another graben has been mapped which is 30–50 m wide and 5–15 m deep and extends for about 600 m south of the flow (Figures 5b and 6), where it abruptly ends. This graben also has freshly broken walls (Plate 2f) and lines up along strike with the ones north of the 1993 flow, although it curves slightly as it cuts through a preexisting constructional hill about 400 m south of the 1993 flow (Figure 6). We also interpret that this graben formed associated with the 1993 CoAxial intrusion. The width of the graben implies that it formed when the top of the dike was at 15–25 m depth. No other 1993 eruptive sites have been identified south of the main 1993 flow. However, when the area was first explored by ROPOS immediately after the T wave swarm, nearly continuous low-temperature venting was observed on the crest of the new flow, in the floor of the graben near the flow (Plate 2f), and along a narrow (~10 m wide) zone of freshly broken and disrupted rock extending at least 4 km farther to the south along strike from the flow [*Embley et al.*, 1995b]. This suggests that the 1993 dike remains quite shallow for at least several kilometers south of the 1993 flow. No hydrothermal activity had been observed along this segment before 1993 (during only a few surveys), and yet immediately after the dike intrusion there were hydrothermal plumes centered over the axis of the CoAxial segment and extending continuously along strike between 46°14′N and 46°33′N, roughly the same extent as the T wave swarm [*Baker et al.*, 1995, this issue; *Embley et al.*, 1995b]. The CoAxial intrusion apparently caused enough deformation and increased permeability above the dike to initiate hydrothermal venting virtually along its entire path. The graben faults are highly permeable conduits that are often the locus of such venting. This venting has declined rapidly (over months to years) in vigor, extent, and temperature since it was

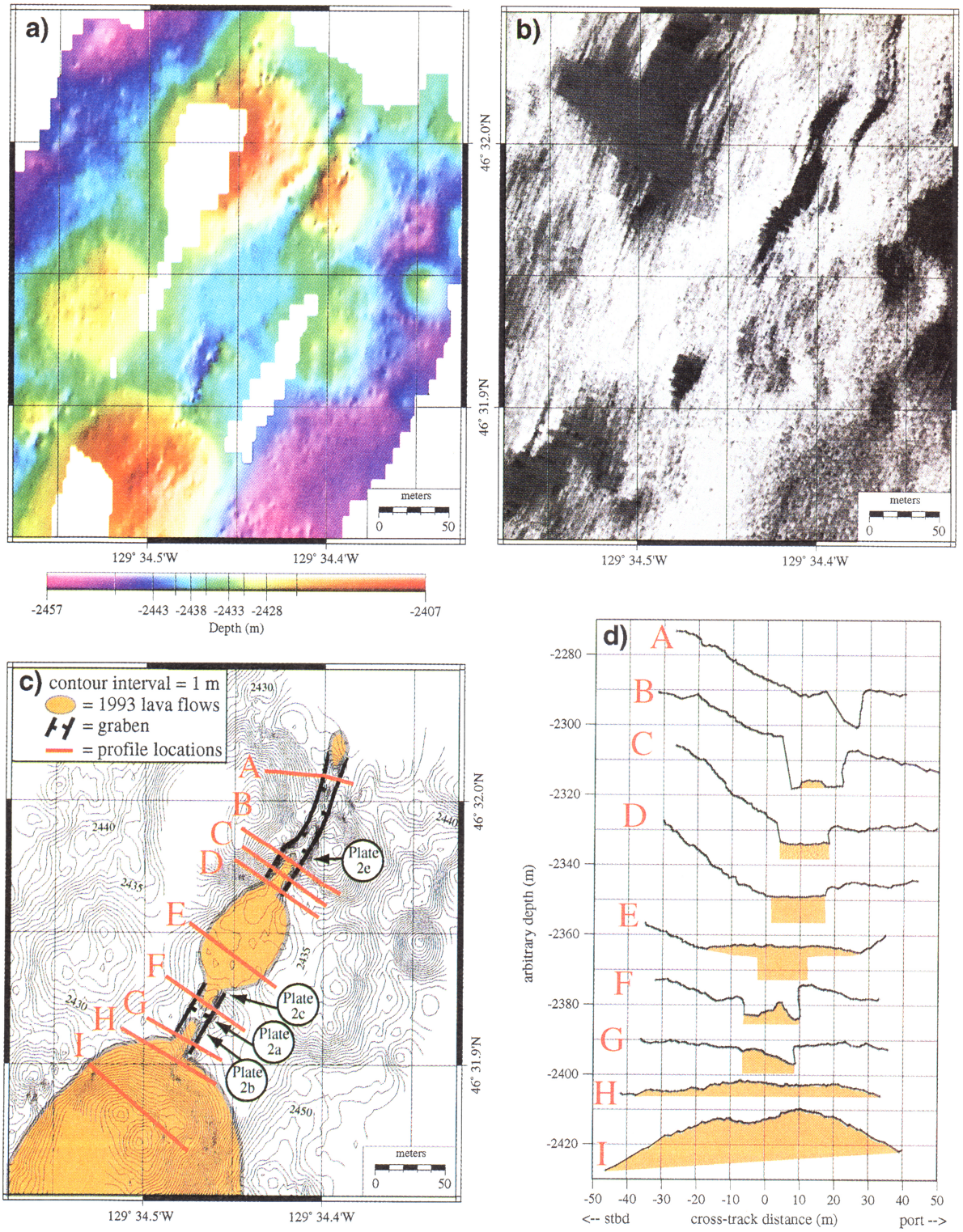

Plate 1. Mesotech and side-scan sonar data from CoAxial Flow site showing the graben at the northern end of the main 1993 lava flow and the first small satellite flow to the north that erupted out of the graben (location is shown in Figure 5b). (a) Mesotech sonar bathymetry from *Alvin* dive 2792 (colored as a function of depth and illuminated from a direction of 115°). (b) AMS-60 side-scan sonar image (illuminated from SE; white is high reflectivity, black is acoustic shadow). (c) Bathymetric contours (1-m interval) of Mesotech data. Geologic mapping of lava flow contacts from *Alvin* dives 2792, 2794, and 2991. Red lines labeled A-I are location of individual Mesotech depth profiles shown in Plate 1d. (d) Individual Mesotech depth profiles (locations are shown in Plate 1c) offset from one another by an arbitrary depth for clarity. Orange areas show 1993 lava and its interpreted extent below each profile. The profiles show, from north to south, the graben with no new lava (profile A), the graben gradually being filled with 1993 lava (profiles B-D), the graben buried by 1993 lava which has slightly overflowed (profile E), the graben reappearing with 1993 lava in its floor between the main flow and the small flow (profile F), which is then buried again by the main 1993 lava flow (profiles G-I).

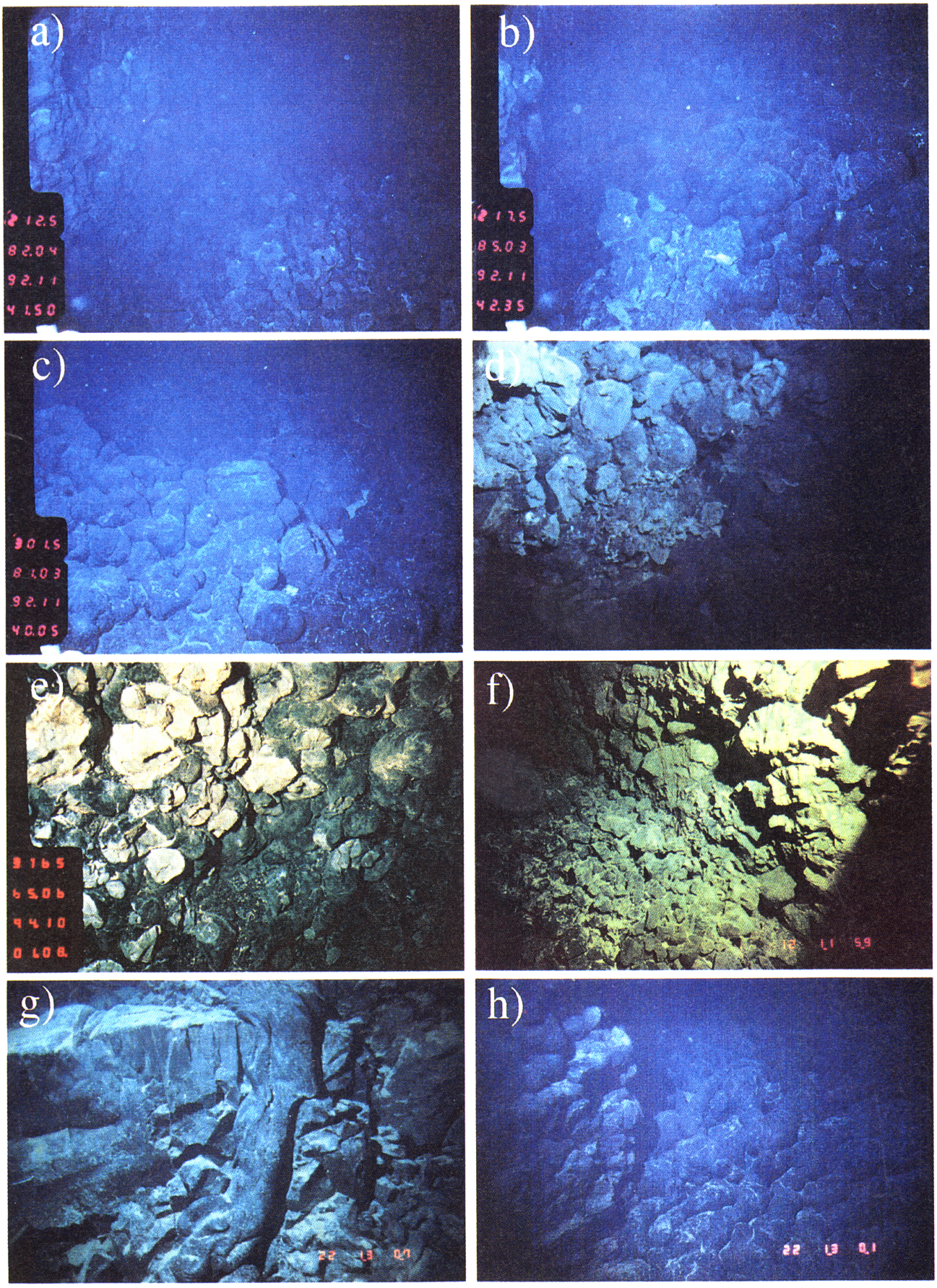
a)
b)
c)
d)
e)
f)
g)
h)

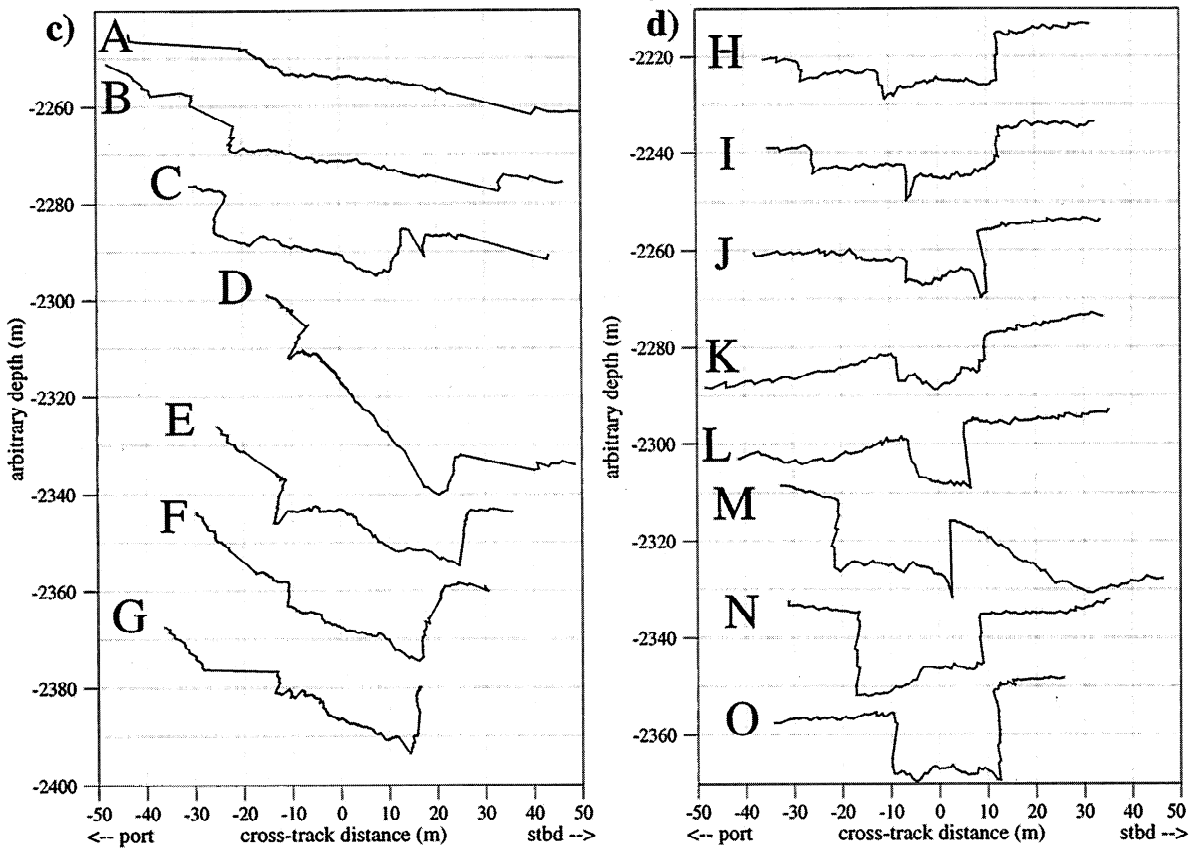

Figure 6. (continued)

first observed [*Embley et al.*, 1994, 1995a; *Baker et al.*, this issue], consistent with the cooling of a near-surface dike [*Wilcock and Delaney*, 1996; *Cherkaoui et al.*, 1997].

The "Floc site" is another area farther south along the CoAxial segment at 46°17′–20′N where low-temperature venting was intense initially and gradually declined over several years. The site was named for the abundant floccular bacteria debris emitted from the vents, apparently from a subsurface bacterial bloom triggered by the intrusion [*Embley et al.*, 1994, 1995b; *Holden et al.*, 1995; *Juniper et al.*, 1995; *Tunnicliffe et*

Plate 2. (opposite) Photographs from submersible *Alvin* showing views of grabens associated with recent eruptions on the Juan de Fuca Ridge. See Figures 5, 6, and 7 and Plate 1 for specific photo locations. Each description is followed by the dive number, time, date, and approximate horizontal dimension of photo. Photos with red numbers in lower left are from *Alvin* bow camera; others are from hand-held cameras; all views are downward oblique. (a) Graben ~50 m north of main 1993 CoAxial lava flow in the gap between the main flow and the first small satellite flow to the north. View looking south: graben wall in upper left, rubble-covered graben floor in lower right (2792, 1141:50 UT, July 6, 1994, 5 m). (b) Same graben as in Plate 2a, but slightly farther south where 1993 lava from main flow begins to fill the graben from the south. View looking south: graben wall at left, old graben floor in foreground, 1993 lava in background (2792, 1142:35 UT, July 6, 1994, 3 m). (c) Same graben as in Plate 2a, but slightly farther north where 1993 lava from first small satellite flow begins to overflow graben. View looking west: older lava in left foreground, 1993 lava in background has filled graben and overflows it in right foreground (2792, 1140:05 UT, July 6, 1994, 3 m). (d) Graben located 1.5 km north of main 1993 CoAxial flow (see Figure 5). View looking north: 1993 lava in lower right was erupted from within the graben and covers the graben floor (2794, 1230 UT, July 8, 1994, 3 m). (e) Freshly fractured graben wall exposing yellow-stained truncated pillows (unsedimented and without biological colonization), ~150 m north of main 1993 CoAxial lava flow. View looking southeast: 1993 lava from first small satellite flow is in floor of graben in lower right (2794, 1001:08 UT, July 8, 1994, 3 m). (f) Freshly broken graben wall (upper right) and rubble covered floor (lower left), both coated with yellow hydrothermal sediment deposited by active diffuse venting, south of main 1993 CoAxial flow (2671, 1159 UT, October 12, 1993, 3 m). (g) Graben wall just south of pillow mound 1, northern Cleft segment. View looking east: 1983–1987 lava erupted out of the graben and overflowed it just to the north (left) and here a single pillow tube of the new lava drapes the graben wall (2262, 1307 UT, August 22, 1990, 3 m). (h) Graben associated with pillow mound 2, northern Cleft. View looking north: 1983–1987 lava at right covers floor of graben and flows up against graben wall at left (2432, 1301 UT, August 22, 1991, 3 m).

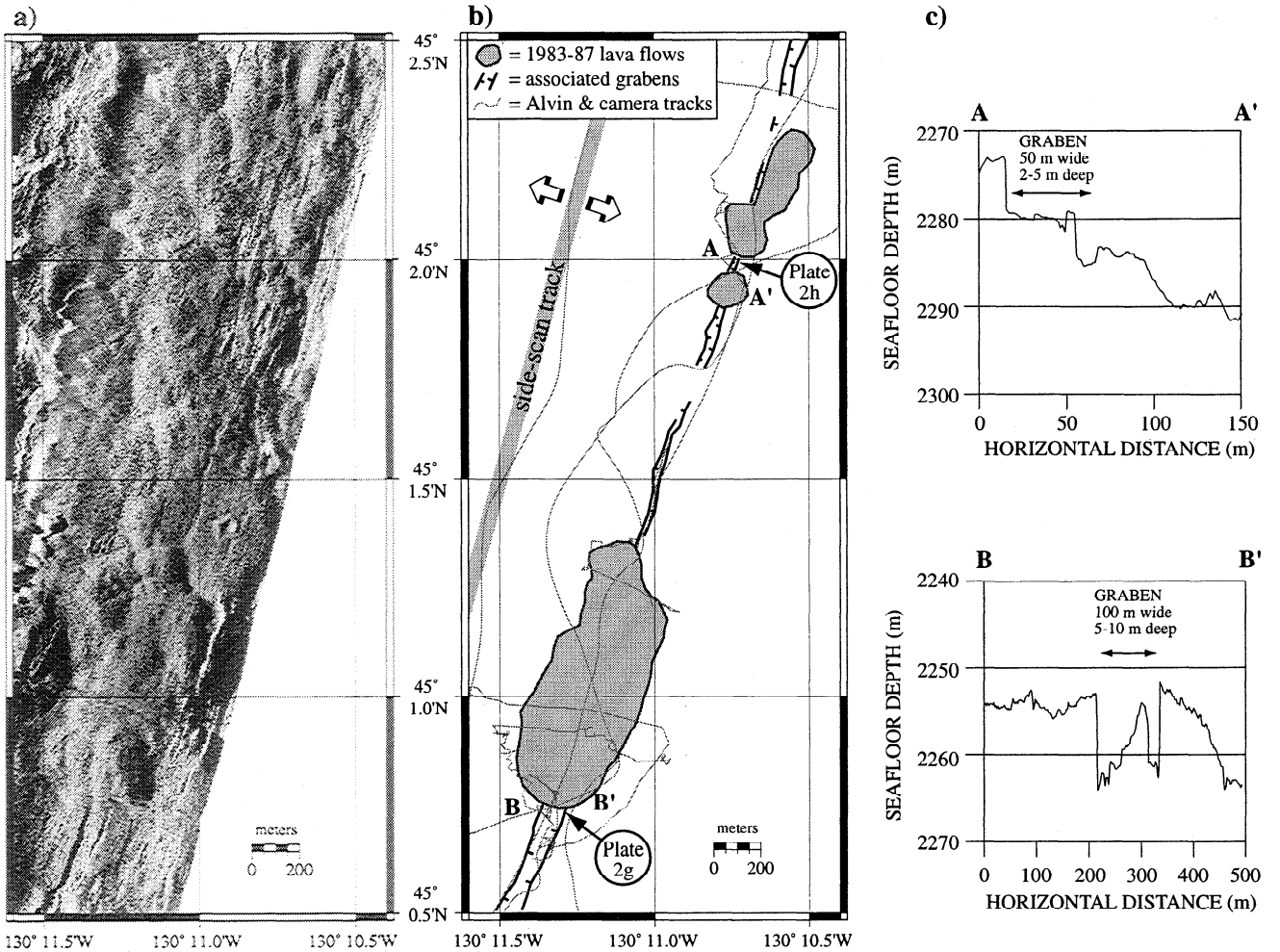

Figure 7. Detailed maps of North Cleft site including pillow mounds 1 and 2 (location is shown in Figure 5c). (a) AMS-60 side-scan sonar image (side-scan track line and illumination directions are shown in Figure 7b; white is high reflectivity, black is acoustic shadow). (b) Geologic interpretation based on side-scan data, camera tow photography, and *Alvin* observations (medium stippled track lines). Grabens that link the recent lava flows are shown in black. (c) Depth cross sections across grabens adjacent to pillow mounds (locations are shown in Figure 7b) from *Alvin* dive 2423 (A–A') and camera tow 89–14 (B–B').

al., 1997; *Baker et al.*, this issue]. At this site, the CoAxial dike apparently reactivated a preexisting, braided fissure/graben system, focusing venting along one graben in particular that is 10–20 m wide and 10–15 m deep, similar in size to the structures at the Flow site. This fissure/graben system at the Floc site, however, clearly predated the 1993 intrusion and probably formed during previous events because older lava lake deposits mantle the graben walls in part of the site. The active venting was focused at the base of the graben walls where extension was probably localized during reactivation. Since the graben is an older reactivated structure, it is difficult to say anything quantitative about the depth of the CoAxial dike here, based on graben width. Qualitatively, however, the fact that the venting was particularly intense and long-lasting, narrowly focused, and nearly continuous along strike at the Floc site suggests that the dike top is unusually shallow and/or wide here compared to most of the rest of the segment. On the basis of the vent fluid chemistry, *Butterfield et al.* [1997] conclude that the depth to the top of the CoAxial dike at the Floc site must be deep enough to provide a high-temperature reaction zone below the seafloor, but *Cherkaoui et al.* [1997] show that a model CoAxial dike can be at relatively shallow depth (~10 m) and still release heat over time through the permeable extrusive layer in a way that is consistent with the plume time series observations.

3.3. Cleft Segment Eruption

The mid-1980s eruption at the north Cleft segment produced a line of isolated pillow lava mounds (1–8 from south to north) along a distance of 17 km, which were also interpreted to be the result of lateral dike injection [*Chadwick and Embley*, 1994; *Embley and Chadwick*, 1994]. Detailed geologic mapping adjacent to several of the pillow mounds during *Alvin* dives 2262, 2432, and 2779 reveals additional evidence of dike-induced graben formation or reactivation. South of the southernmost pillow mound ("mound 1") a graben that is 100 m wide and 5–10 m deep extends southward for at least 1 km (Figures 5c and 7 and Plate 2g). This graben probably predated the mid-1980s eruption, based on the minor but significant sediment accumulation on its bounding walls during *Alvin* dive 2262 in 1990. It is possible its formation was associated with the

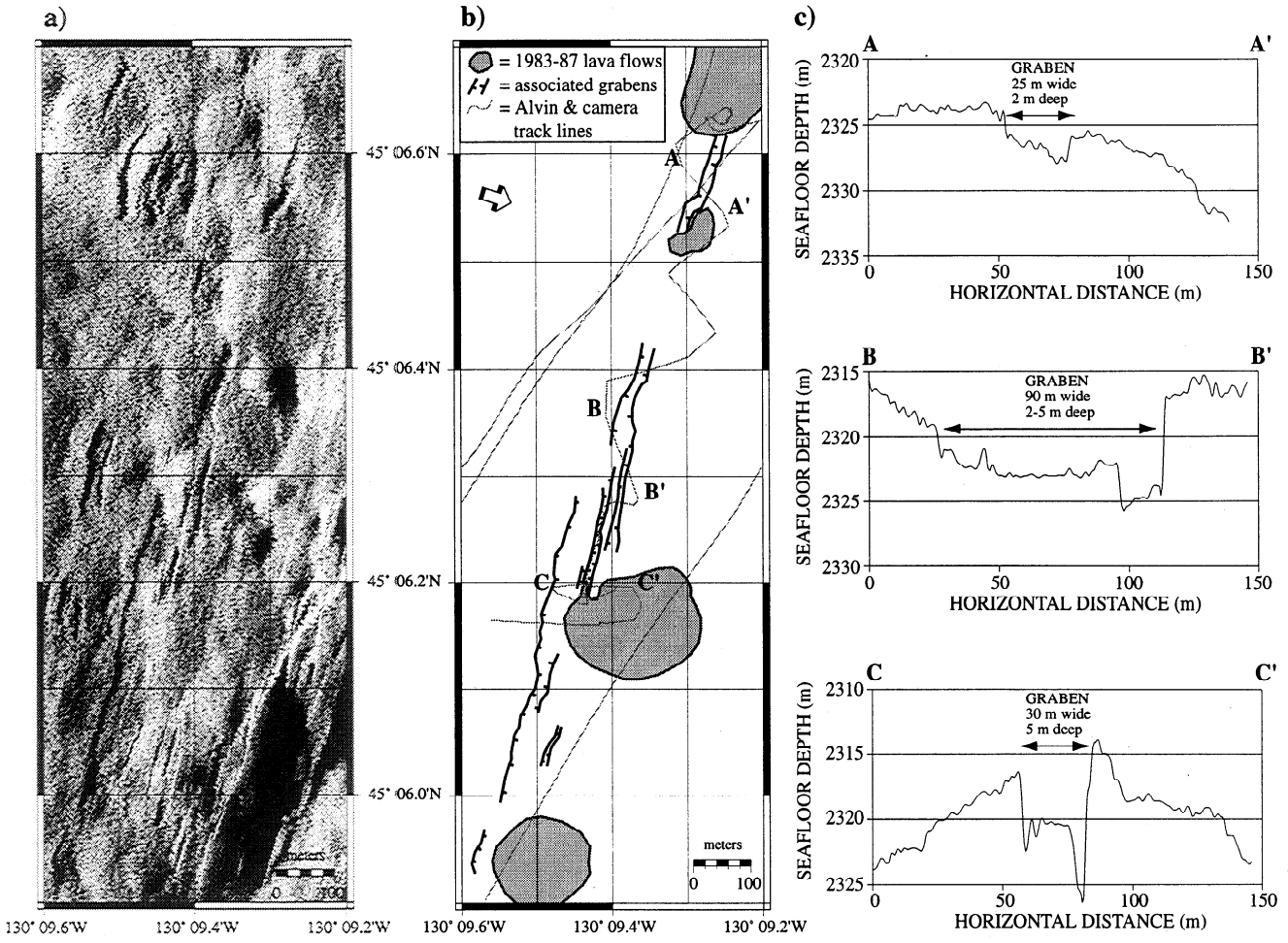

Figure 8. Detailed maps of North Cleft site between pillow mounds 5 and 6 (location is shown in Figure 5c). (a) AMS-60 side-scan sonar image (side-scan illumination direction is shown by arrow in Figure 8b; white is high reflectivity, black is acoustic shadow). (b) Geologic interpretation based on side-scan data, camera tow photography, and *Alvin* observations (medium stippled track lines). Grabens that link the recent lava flows are shown in black. (c) Depth cross sections from *Alvin* dive 2779 (locations shown in Figure 8b) showing variation of graben shape along strike.

eruption of a young sheet flow at north Cleft (at least a few years before the pillow mound eruption) because the graben is also located along the northern continuation of the fissure system that fed this earlier eruption [*Embley and Chadwick*, 1994]. In any case, the dike that fed the pillow mound eruption probably underlies and reactivated the graben because low-temperature hydrothermal vent sites were located within it, and these vent sites declined rapidly between 1989 and 1991 (consistent with the rapid cooling of an underlying dike and similar to the CoAxial vent sites). In addition, the "mound 1" lava flow was clearly erupted directly out of the graben (Figure 7).

A second graben was mapped during *Alvin* dive 2432 adjacent to "mound 2"; this one, 50 m wide and 2–5 m deep, has a 2- to 5-m horst in the middle and is floored with new lava (Plate 2h and Figure 7). The lavas of "mound 2" clearly erupted out of the graben and then flowed downslope to the east (Figure 7). The faults bounding this graben appeared to be freshly broken, so we interpret that this graben formed during the mid-1980s eruption.

Grabens south of "mound 6" were mapped on *Alvin* dive 2779. They are 20–80 m wide and up to 5 m deep and extend discontinuously for at least 800 m along strike (Figures 5c and 8). Here a series of small new lava flows were erupted out of, and are linked along strike by, a system of fissures and grabens which clearly stand out visually in the older but mostly unfractured pillow lavas. The grabens vary in size and apparent age along strike; the smaller ones in the north appear to be new, whereas the larger ones in the south are probably reactivated structures (Figure 8).

In all of these cases at north Cleft, it is clear that the recent pillow mounds erupted directly out of the grabens or their along-strike extensions, strongly suggesting that the grabens were formed or reactivated by the near-surface stresses created by the dike just before it erupted at the surface. The widths of the Cleft grabens suggest that they formed when the underlying dike was 10–50 m below the surface, again relatively shallow.

The southern end of the Cleft segment is characterized by a prominent graben (from which the segment gets its name) that is 15 km long, 30–60 m wide, and 10–30 m deep [*Normark et al.*, 1986; *Kappel and Normark*, 1987]. This graben bisects the floor of the axial valley and is interpreted to be the eruptive fissure for voluminous, young sheet and lobate flows that cover the entire valley floor between 44°35'N and 44°43'N [*Normark*

et al., 1983, 1986, 1987; *Kappel and Normark*, 1987]. Lava drainback features are common along the cleft [*Holcomb and Morton*, 1986; *Holcomb et al.*, 1987], much like along the axial summit graben of the East Pacific Rise [*Haymon et al.*, 1991; *Fornari et al.*, this issue]. High-temperature hydrothermal vents are located at three sites along the graben at south Cleft, which were probably local centers of eruptive activity [*Normark et al.*, 1983, 1986]. This is yet another example of a narrow, deep graben associated with a recent eruption (of unknown age, in this case) that apparently formed when the dike that fed the eruption was within tens of meters of the surface.

3.4. Graben Formation During a Single Event Versus Multiple Events

The mapping results described above indicate that some of the grabens associated with recent eruption sites on the JdFR probably formed during the most recent volcanic events (CoAxial/Flow site, Cleft/mound 2), others were probably preexisting structures that got reactivated (CoAxial/Floc site, Cleft/mound 1), and some sites have both new and older structures (Cleft/mound 6). Where grabens appear to have been reactivated, this implies that dikes have intruded along nearly the same axis and reactivated the same graben faults more than once. Perhaps new dikes sometimes use the zones of weakness created by earlier dikes as structural guides, particularly when the intrusions occur closely spaced in time [*Wilson and Head*, 1988]. This may not be uncommon since in ophiolites it is often observed that younger dikes have split older ones [*Pallister*, 1981]. On the other hand, it is unlikely that the preexisting graben faults guided the intrusion path of a subsequent dike and thus caused the grabens to be reactivated, since the faults are shallow structures (only extending between the dike tip and the surface [*Rubin*, 1992]) and would not have much influence on a dike originating at greater depth. On fast spreading ridges like the EPR, where intrusions are more narrowly focused within the neovolcanic zone, the reactivation of graben structures by multiple intrusion events may be even more common. On intermediate spreading ridges like the JdFR, however, this must only happen occasionally because the neovolcanic zone is typically up to 0.5–2 km wide. For example, at the CoAxial Flow site, two lava flows were erupted within 12 years and are separated by 700 m across axis [*Chadwick et al.*, 1995].

4. Comparison to Subaerial Examples and Implications

All of the grabens associated with seafloor eruptions discussed in section 3 are within a similar size range, with widths of 10–100 m and depths of 5–15 m (Table 1). We interpret that at least some of them were entirely formed during the most recent dike intrusions, and therefore their depth equals the amount of subsidence during one event. On the other hand, geodetic observations from rift zones on land have documented examples of dike-induced graben formation on a significantly different scale: widths up to 1–6 km and subsidence usually only 0.5–1.5 m (Table 2). This comparison suggests that dike-induced grabens on the seafloor tend to be narrower and deeper than their subaerial counterparts. How general is this distinction, and what might it mean?

First, let us consider how valid this distinction might be. Could wide, shallow grabens have also formed during the Cleft and CoAxial eruptions in addition to the observed narrow, deep ones? Recent fracturing can be obvious on the seafloor in some cases, but it depends on how much fracturing there has been before (this is also true on land; some reference surface is needed to identify recent changes, like a recent volcanic ash layer, a paved road, or a young unfractured lava flow). Wide, shallow grabens might be difficult or impossible to recognize on the seafloor without the kind of precise deformation monitoring available on land. However, if a wide graben formed and relieved the local tensile stress by inelastic deformation when the dike was deep, a narrow one would probably not form in

Table 1. Dimensions of Grabens Associated With Recent Eruptive Sites on the Juan de Fuca Ridge

Graben Location	New or Old Faults?*	Graben Width, m	Graben Depth,† m	Minimum Graben Length, m	Estimated Depth to Dike Top,** m	Estimated Dike Width,†† m
CoAxial segment: north of 1993 Flow	new	10–20	5–15	200–2000	5–10	1.5–3
CoAxial segment: south of 1993 Flow	new	30–50	5–15	600	15–25	1.5–3
CoAxial segment: Floc site	old	10–20	10–15	1000	5–10	3
North Cleft segment: mound 1	old	100	5–10	1000	50	3
North Cleft segment: mound 2	new	50	2–5	500	25	3
North Cleft segment: mound 6	both	20–80	1–5	800	10–40	1.5

* Based on appearance of fault scarps (degree of sediment accumulation, biological colonization).

† Graben depth is assumed to be equal to the subsidence that occurred during the most recent dike intrusion if the faults appear to be new.

** Estimated depth to dike top is equal to half the graben width, a general relation derived from mechanical modeling results [*Pollard et al.*, 1983].

†† Estimated dike width is equal to 1.5 times a crude estimate of cumulative extension observed at the surface across cracks and faults, a relation from physical model results [*Mastin and Pollard*, 1988].

Table 2. Dimensions of Grabens Associated With Recent Dike Intrusion Sites in Iceland and Afar

Graben Location	New or Old Faults?	Graben Width, m	Graben Subsidence During This Event, m	Measured Horizontal Estimated Depth to Dike Top,* m	Measured Horizontal Extension at the Surface, m	Estimated Dike Width,* m
Krafla, Iceland: north rift zone (Kelduhverfi)	old	6000	1.0	1500	2.4	1.5
Krafla, Iceland: south rift zone (Namafjall)	old	1500	1.5	1250	1.0	2.6
Asal-Ghoubbet rift, Djibouti (Afar)	old	3500	0.9	1250	1.9	1.5–3.0

* Estimates of depth to dike top and dike width are based on mechanical modeling results which best fit measured geodetic data during specific intrusions; results for Iceland are from *Rubin* [1992], and estimates for Afar are from *Stein et al.* [1991].

addition when the dike neared the surface (the stress field would have already changed to compression between the first graben faults [*Rubin*, 1988]). Therefore the presence of a narrow graben implies that it accommodated the majority of the extension at the surface during that particular event. An eruptive fissure can still open within the floor of a newly formed graben (even though the graben caused the local stress field to turn compressive) if the magmatic pressure inside the dike is still greater than the local ambient stress. On land, dike-induced grabens have been documented at a wide range of scales [*Pollard et al.*, 1983], but it is the examples from spreading centers on land (e.g., Iceland and Afar) that we are most interested in for direct comparison with the JdFR, and these have been uniformly wide and shallow in size (Table 2).

What is the significance then of this apparent distinction between grabens on land and on the seafloor? That graben widths are narrower for the events on the JdFR indicates that they formed when the dike below them was much shallower (according to the model results outlined in section 2). This would also suggest that the local stress state on the JdFR needed a relatively high stress perturbation from the dike (when it was shallow) before surface faulting and graben formation could occur. On the other hand, in north Iceland, wider grabens formed when the dikes were deeper, apparently because the local horizontal compressive stresses had been gradually lowered by over 100 years of remote tectonic extension without any volcanic activity. In such a state, preexisting normal faults were near a state of incipient slip and needed only a small stress perturbation from the dike (when it was deep) to trigger faulting at the surface [*Rubin*, 1992]. This implies that during the Cleft and CoAxial dike intrusions the JdFR had a higher horizontal compressive stress across the rift axis compared to north Iceland during the Krafla rifting episode, even though the spreading rate is higher on the JdFR (6 versus 2 cm/yr), which would tend to lower the ridge-normal compressive stress at a faster rate.

A contributing factor to the relatively high horizontal compressive stress at both Cleft and CoAxial may be that both sites have had other recent eruptions, probably within a decade of the most recent eruptions discussed above. At north Cleft, geologic mapping and side-scan sonar data indicate that a young sheet flow was erupted several years before, and just south of, the 1983–1987 pillow mounds [*Embley and Chadwick*, 1994]. At CoAxial, repeated multibeam sonar surveys together with bottom observations document two previous eruptions along the segment between 1981 and 1991, a northern one directly east of the Flow site and a southern one just west of the Floc site [*Chadwick et al.*, 1995; *Embley et al.*, 1995a]. The earlier eruptions at each site must have increased the horizontal compressive stress, perhaps making the most recent intrusions more likely to form narrow grabens. *Rubin* [1992] used the same reasoning to explain why a graben that formed south of Krafla was narrower than one that formed to the north; there had been more recent intrusive events to the south.

Previous studies on land have also noted that when multiple intrusions occur in the same area, later events are more likely to lead to eruptions at the surface, presumably because the earlier events had increased the horizontal compressive stress perpendicular to the rift axis, which forced later dikes to be intruded with a higher magmatic pressure [*Ando*, 1979; *Björnsson*, 1985; *Einarsson*, 1991]. This was probably also a factor affecting the recent JdFR eruptions. Furthermore, the previous locations of intrusions along a rift zone can cause the horizontal compressive stress to vary along strike [*Björnsson*, 1985; *Rubin*, 1992]. On the JdFR, for example, it is remarkable that the 1993 CoAxial dike intruded for 60 km along strike and apparently approached near the surface at the Floc site (directly adjacent to the southern 1981–1991 lava flows), and then ended up erupting directly adjacent to the northern 1982–1991 lava flow [*Chadwick et al.*, 1995; *Embley et al.*, 1995a]. There was also enhanced hydrothermal venting from the dike at these two sites [*Baker et al.*, this issue]. Locally higher compressive stress adjacent to the previous extrusions may have forced the 1993 CoAxial dike closer to the surface in those locations. At both Cleft and CoAxial, the dikes also intruded down a topographic gradient and erupted near the distal ends of the segments [*Embley et al.*, 1994].

Another obvious difference between dike intrusions on the MOR and on land is that the oceanic crust at a spreading axis is thinner and the depth of neutral buoyancy for magma is shallower [*Ryan*, 1993]. This would tend to limit dike intrusions to shallower depths than within thicker crust on land. Having thinner crust effectively limits how deep a dike can potentially extend and thus favors the formation of narrower grabens.

The relationship between subsidence and horizontal extension across a normal fault bounding a graben is simply a function of the dip angle of the fault. The greater depth of the grabens we have mapped on the JdFR (5–15 m), as compared to vertical displacements during single intrusions on land (0.5–

1.5 m), suggests that on the JdFR either the underlying dikes are wider (providing more extension) or the bounding faults of the grabens are steeper (providing more subsidence per unit extension) or both. Another factor contributing to their greater depth may be the incremental growth of some grabens during multiple events, although we interpret that at least some were formed during a single event.

The dike widths estimated for the JdFR intrusions (Table 1) are on the same order as model estimates for the north Iceland intrusions (Table 2), so it seems more likely that the graben faults on the JdFR are steeply dipping (perhaps average dips of 80°). *Mastin and Pollard* [1988] showed that dike-induced graben faults are likely to be near-vertical at the surface since they begin as simple tension cracks and gradually link up with other fractures and a zone of distributed shear between the dike top and the surface (Figure 2), and this is consistent with field observations in subaerial volcanic rift zones [*Opheim and Gudmundsson*, 1989]. Since the JdFR grabens are narrow, their bounding faults do not extend very deep (probably <100 m), and their steeply dipping, shallow parts will be a significant percentage of their total length. Thus it may be easier for narrow grabens to be deeper.

5. Implications for the East Pacific Rise: Is the Axial Summit "Caldera" Really a "Graben"?

In many areas, the crest of the fast spreading East Pacific Rise (EPR) is marked by a narrow, linear trough that usually ranges in size from 5–10 m deep and 40 m wide up to 30–50 m deep and 200–400 m wide. In a few locations, the trough is even larger, up to 50–100 m deep and 0.5–2.0 km wide, but in some of these cases a narrower trough is nested within the larger one. Fluid lava is erupted from within the axial trough and commonly only forms a thin upper crust before its still molten interior rapidly drains away, leaving extensive areas of lava collapse (including lava pillars, roof remnants, and collapse pits). In locations where it is relatively wide, the depression is clearly bounded by near-vertical fault scarps, but where it is narrower, the edges of the trough are obscured by the products of recent eruptions and drainback.

The terminology used to describe the axial trough on the EPR has changed over time and is currently under debate because the origin of the trough is controversial and different names have specific genetic implications. Until recently, the axial trough was referred to as the "axial summit graben" (ASG), regardless of its scale [*Lonsdale*, 1977; *Hekinian et al.*, 1983; *Ballard et al.*, 1984; *Choukroune et al.*, 1984; *Renard et al.*, 1985; *Gente et al.*, 1986; *McConachy et al.*, 1986; *Macdonald and Fox*, 1988; *Auzende et al.*, 1996]. On the other hand, *Lonsdale* [1977] proposed that the summit trough probably formed by "caldera collapse" after "relief of magma pressure by an eruption," and later *Haymon et al.* [1991] argued that the term "axial summit caldera" (ASC) should be used instead of "axial summit graben" for all summit troughs. More recently, a twofold nomenclature was proposed by *Fornari et al.* [this issue], who assert that the trough should be called "axial summit caldera" where it is narrow (<200 m), and "axial summit graben" where it is wide (>200 m). In contrast, *Lagabrielle et al.* [1996] argue that only the largest axial troughs (0.5–2.0 km wide) are formed by caldera collapse. Below, we present arguments to support an alternative interpretation that the axial trough on the EPR is fundamentally a "graben" rather than a "caldera," regardless of its size, and discuss how it may relate to the other intrusion-related grabens described above from the JdFR.

A caldera is defined as a depression formed by "collapse of the roof of a magma chamber owing to removal of magma by eruption or by subterranean withdrawal" [*Bates and Jackson*, 1984, p. 70]. However, this definition seems physically unrealistic, at least for the narrow (<200 m) axial troughs on the EPR. The latest geophysical models envision the "magma chamber" beneath the EPR as a thin lens of mostly liquid magma (<100–500 m thick and 1–2 km wide, at 1–2 km depth) over a more extensive body of partial melt and crystal mush [*Sinton and Detrick*, 1992]. The size and shape of the narrow axial troughs (Figure 9a) are inconsistent with the notion of them forming by magma withdrawal from the much wider and deeper magma lens, which would form a wider, more circular or elliptical depression at the surface [*Ryan et al.*, 1983]. Where the axial trough is narrow, could the withdrawal be into shallower conduits instead? Eruptions within the axial trough are fed from the magma chamber to the surface by narrow dikes. Since the erupted lava tends to pond within the confines of the preexisting trough, it also tends to drainback into the dike during an eruption's waning stages. This drainback often leads to collapse of the thin upper crust on a new lava flow within the trough. However, this process is not "caldera collapse"; it is not a structural collapse of the magma chamber roof but merely the failure of unsupported lava crust at the surface. In fact, if an axial trough were not present to begin with, it seems unlikely that one could form by surficial lava drainback alone because thin sheet flows could then spread outward from the vent and drainback would be minor. Since eruptions on the EPR tend to erupt into a preexisting trough, a key question is therefore how does the trough form in the first place?

In locations where the axial trough is relatively wide, it is clearly bounded by near-vertical fault scarps, but in locations where the trough is narrow (for example, 9°–10°N on the EPR), its edges are defined by lava drainback and collapse from recent eruptions and no faults are evident [*Fornari et al.*, this issue]. A possible explanation for this is that where lava collapse features are dominant, they may mask and bury the structures that physically define the trough. Between 9° and 10°N on the EPR, the edges of the axial trough in map view are scalloped, sinuous, and even jagged on a scale of meters to tens of meters (Figure 9b). This fine-scale irregularity is simply where the remnants of lava crust have collapsed into the axial trough versus where they remain supported by pillars or walls [*Fornari et al.*, 1990, this issue]. However, on a scale of kilometers to tens of kilometers, the axial trough is long, narrow, linear, and en echelon (Figure 9a), all suggestive of the characteristic shape and dimensions of structural features such as cracks, dikes, or grabens. It is this continuity over long distances that argues for structural control; the effects of surficial collapse processes would vary widely from location to location unless they were constrained within a preexisting structure. In other words, the irregularities observed at a fine scale may be superimposed on a underlying structural control at a larger scale. The continuity of processes along the EPR crest also argues for structural control; it is well-documented that grabens are associated with dike intrusions and that grabens define the axial trough where it is relatively wide [*Renard et al.*, 1985; *Gente et al.*, 1986]. Why not also where it is narrow?

Grabens commonly form above intruding dikes in volcanic rift zones on land, and they have been documented adjacent to recent submarine eruptions on the Juan de Fuca Ridge. There is

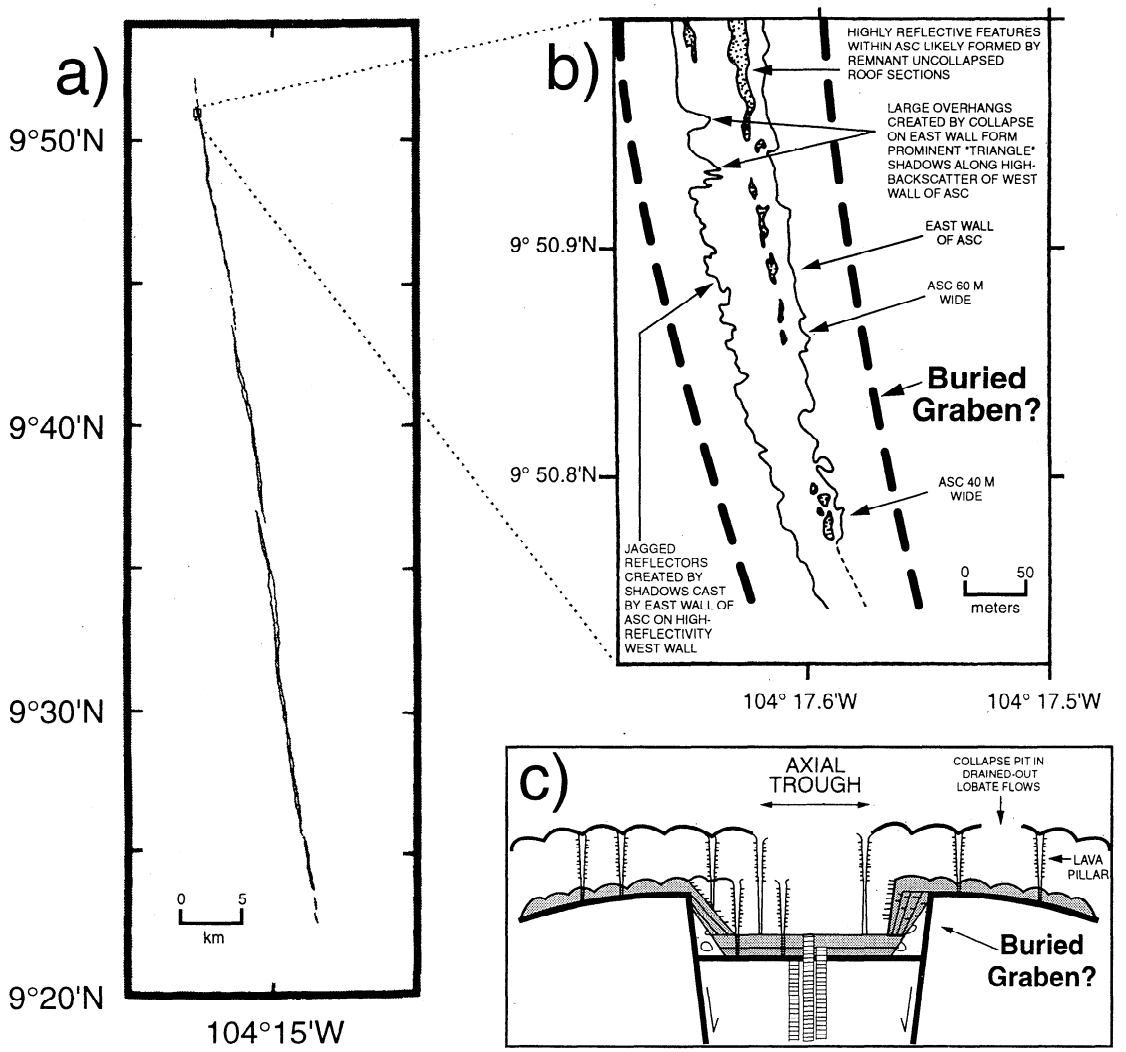

Figure 9. (a) The "axial summit caldera" at 9–10°N on the East Pacific Rise (EPR), from *Haymon et al.* [1991]. (b) Interpretive sketch of a sonar image showing irregular margins of the axial trough on the EPR, modified from *Haymon et al.* [1991]. The location of a hypothetical buried graben has been added; the graben faults do not crop out at the surface but nevertheless control the overall location and dimensions of the trough. (c) Cartoon cross section of an axial trough on the EPR showing hypothetical buried graben faults associated with dike intrusion controlling the location of the depression.

no reason why this process should not also be active on the EPR. One reason some observers have called the axial trough a "caldera" is that it appears to be "volcanic" rather than "tectonic" (the term "volcanic caldera" is often contrasted with "tectonic graben"). This is because lava collapse features can be extensive within the narrowest axial troughs and often faults are not observed at their edges. Implicit in this view is the assumption that a "tectonic graben" must form in the absence of volcanism, and since many parts of the EPR appear to have had recent eruptions, then it is assumed that the axial trough cannot be a graben. However, as described in section 2, grabens can form during volcanic events, and therefore this "volcanic" versus "tectonic" dichotomy is not absolute. In fact, since the axial trough is the locus of most dike intrusions on the EPR, one should expect that these dikes would produce graben subsidence directly above them. Thus dike-induced graben formation is a viable mechanism to initiate and maintain the axial trough along the crest of the EPR.

The arguments above support the hypothesis that the "axial summit caldera" on the EPR is fundamentally a graben. The key difference in the interpretations is that graben faulting would occur during dike intrusion and before an eruption starts, whereas caldera subsidence would occur after an eruption. Since graben faulting occurs before the eruption of lava, the evidence of faulting may often become obscured, especially where the trough is narrow; the erupted lavas would tend to bury and mask the faults of the axial trough with overflows and lava subsidence formations that adhere to the walls during lava drainback (Figure 9c). In this way, the fault scarps may become buried beneath tens of meters of overflows and may lie tens of meters outside the present margins of the axial trough whose walls have grown inwards with successive eruptions. This may explain how lava can be transported up to 50–100 m outside the axial trough through subseafloor "tubes and channels" [*Haymon et al.*, 1993]. At the high-stand of an eruption, lava could be introduced into the drained-out, hollow interiors of previous lobate overflows immediately adjacent to the trough (Figure 9c). At any one place on the EPR, the detailed structure of the axial trough is probably rarely the consequence of just one diking event but is more likely the sum of multiple faulting and

eruption episodes because of the high frequency and narrow focusing of dike intrusions there. Therefore the presence or absence of an axial trough does not necessarily imply evidence of a long-term cycle of alternating volcanic/tectonic phases. Each intrusive/eruptive event adds its own contribution to the evolving structure of the axial trough: one may deepen it by graben subsidence, the next may fill it completely with new lava. On the other hand, the observation that the widest axial troughs tend to be on segments with relatively low magma budgets [*Lagabrielle et al.*, 1996] is consistent with the idea that they form by relatively infrequent dike intrusions which usually do not reach the surface.

If dike-induced graben subsidence forms the underlying structural control for the axial trough on the EPR, then the most common dimensions of the axial trough (where it is relatively narrow and associated with relatively high magma supply) support the observation from the JdFR that dike-induced grabens on these mid-ocean ridges tend to be narrower and deeper than those observed on land.

6. Discussion and Conclusions

We interpret that the grabens associated with recent eruption sites on the JdFR formed or were reactivated during the intrusion of the dike that fed the eruptions because (1) mechanical models and volcano monitoring have established a direct connection between dike intrusion and graben formation, (2) the grabens on the JdFR line up with the linear eruptive vents for the flows and "link" larger flows to smaller ones along strike, (3) the smallest lava flows are confined within the grabens and clearly erupted out of them, and (4) time-dependent (months to years) low-temperature venting found along the grabens is evidence of a cooling dike at shallow depth directly beneath them. Modeling suggests that the graben faulting occurs during dike intrusion and is over before the dike reaches the surface. Therefore, when the dike finally reaches the surface and eruptive fissures open in the floor of the graben, lava may bury it partially or completely, depending on how much is erupted. On the JdFR we have found that grabens are commonly preserved at one or both ends of a new lava flow, along the strike of the neovolcanic zone. The unburied grabens thus trace the path of the subsurface dike that fed the eruption. Such grabens may accommodate much of the near-surface extension during individual seafloor-spreading events and are therefore primary conduits for diffuse hydrothermal venting immediately after intrusion, while the dike is cooling.

Our observations suggest that dike-induced grabens formed during individual intrusion events on the intermediate to fast spreading MOR (the JdFR and EPR) tend to be narrower and deeper than examples from slow spreading ridges on land (Iceland and Afar). Why might this be the case and what is its significance? Modeling results show that narrow grabens form when the underlying dike is shallow and the tensional stress perturbation required for faulting is high. In other words, the narrow grabens on the JdFR and EPR imply that the ambient stress state on these ridges is not typically "primed" for faulting; there is not enough time between spreading events for plate motion to increase the ambient tensional stress to near-critical levels where faulting could be triggered by a small stress perturbation (potentially from a deep dike, which would form a wide graben). This suggests two things: first, dikes that intrude in this environment must have a relatively high internal pressure to overcome the ambient stress, and second, that dike intrusions on the JdFR and EPR occur much more frequently than in slow spreading environments, even relative to the spreading rate. In other words, a higher percentage of the total extension is accommodated by diking than by faulting at the fast spreading end of the spectrum, whereas at slow spreading ridges faulting plays a larger role. This varying relative contribution from diking and faulting indicates that the frequency of eruptions on the MOR increases nonlinearly with spreading rate; if it increased linearly, the ratio of volcanism to tectonism (and the resulting ridge morphology) would be the same at all spreading rates. Instead, there are much more frequent eruptions at the fast spreading end of the spectrum [*Perfit and Chadwick*, 1997]. This is apparently due to the fact that magma reservoirs can only exist in a steady state on ridges that spread at a rate above about 50 mm/yr [*Phipps Morgan and Chen*, 1993a, b] and the availability of magma obviously has a strong influence on eruption frequency.

This difference in graben widths is probably more a function of the fast versus slow rate of spreading in the different environments, as opposed to the difference of seafloor versus land, although crustal thickness may also be a factor. In a slow spreading environment, the ridge is relatively magma-starved, leading to long time intervals between events, which promotes the formation of wide, shallow grabens when diking does occur. Because of the low magma supply, critical stress levels for extensional failure may often be reached without magma input, and normal faulting would occur instead. Of course, this situation could also occur on a fast spreading ridge like the EPR at times or in locations of low magma supply (where grabens $\geq$0.5 km wide exist), but typically the magma supply there is relatively high, leading to short time intervals between events, which effectively means that diking will almost always occur before the stresses reach the critical level for normal faulting [*Parsons and Thompson*, 1991]. This promotes the formation of narrow, deep grabens above dike intrusions and also repeated diking within a very narrow zone. At intermediate rate spreading centers, it may be some combination of these two end-members, even varying from segment to segment, depending on the local magma supply. Both the Cleft and CoAxial segments on the JdFR have had multiple eruptive events within the last two decades and so were pushed toward the "fast spreading" end of the spectrum in terms of having relatively high levels of ambient compressive stress and thus were in a state conducive to the formation of narrow grabens during the most recent events. At other times, or at other locations on the JdFR (or EPR), wider grabens may form when the frequency of intrusions is lower, even involving the faults bounding the axial valley.

The difference in graben widths noted above could also be partly related to the different tectonic settings between the submarine ridge crests and subaerial spreading environments. Since the brittle crust is thinner at intermediate to fast spreading ridges, dikes there are constrained to be intruded at shallower depths, and this narrows the width of the zone of potential faulting above a dike.

Are there any examples of dike-induced graben formation on submarine slow spreading MORs? Certainly many normal faults and grabens exist on the Mid-Atlantic Ridge [*Karson et al.*, 1987; *Kong et al.*, 1988; *Mutter et al.*, 1988; *Head et al.*, 1996], but it is difficult to associate specific structures with individual intrusion events, because (1) no historical eruptions have been documented, (2) the neovolcanic zone is wider and less focused across axis, (3) it is harder to differentiate purely tectonic from dike-induced structures, and (4) axial volcanic ridges are the product of multiple events which coalesce, overlap, and often produce small seamounts which bury associated structures

[*Smith and Cann*, 1993]. So, although we speculate that grabens which form on submarine slow spreading ridges tend to be wider than those on intermediate and fast ridges (as observed on land), there are not enough data from the seafloor to provide specific examples. Nevertheless, dike intrusion has previously been suggested as contributing to the morphology of the axial valley [*Davis*, 1984], and recent high-resolution side-scan sonar data show a general association between grabens and young axial volcanic ridges [*Head et al.*, 1996].

Björnsson [1985, p. 10,160] stated (referring to rifting in Iceland) "The amount of available mobile magma is very likely one of the most important factors that control the periodicity of rifting [diking] episodes ... ." It also profoundly affects the ambient stress state in the vicinity of the ridge crest and controls the character of dike-induced faulting, which is a major contributor to the fine-scale morphology of mid-ocean ridge crests.

Acknowledgments. We thank the *Alvin* dive observers who made key observations or collected some of the Mesotech sonar data presented in this paper: Mike Perfit, H. Paul Johnson, Cindy Van Dover, and Julia Getsiv. The photograph in Plate 2d was taken by Mike Perfit. We also wish to thank the *Alvin* group and the helpful crews on the *Atlantis II* and NOAA ship *Discoverer*. Thanks also go to John Delaney for inviting our participation during the 1993 *Alvin* dives at CoAxial. We are indebted to Dan Scheirer for writing and sharing with us his Mesotech data processing software. Stuart Sides and Miguel Valasco (USGS) provided expert side-scan data processing and helpful advice in using USGS-MIPS software. Special thanks to Paul D. Johnson for invaluable assistance with the figures. This paper benefited from thoughtful reviews by John Chen, Jeff Karson, and Dan Fornari (who spent considerable time and effort debating the issues and interpretations with us in a friendly and professional spirit). This research was supported by the NOAA/VENTS Program. PMEL contribution 1845.

References

Abdallah, A., V. Courtillot, M. Kasser, A. Y. Le Dain, J. C. Lepine, B. Robineau, J. C. Ruegg, P. Tapponnier, and A. Tarantola, Relevance of Afar seismicity and volcanism to the mechanics of accreting plate boundaries, *Nature*, *282*, 17–23, 1979.

Ando, M., The Hawaii earthquake of November 29, 1975: Low dip angle faulting due to forceful injection of magma, *J. Geophys. Res.*, *84*, 7616–7626, 1979.

Auzende, J. M., et al., Recent tectonic, magmatic, and hydrothermal activity on the East Pacific Rise between 17°S and 19°S: Submersible observations, *J. Geophys. Res.*, *101*, 17,995–18,010, 1996.

Baker, E. T., G. J. Massoth, and R. A. Feely, Cataclysmic hydrothermal venting on the Juan de Fuca Ridge, *Nature*, *329*, 149–151, 1987.

Baker, E. T., J. W. Lavelle, R. A. Feely, G. J. Massoth, S. L. Walker, and J. E. Lupton, Episodic venting of hydrothermal fluids from the Juan de Fuca Ridge, *J. Geophys. Res.*, *94*, 9237–9250, 1989.

Baker, E. T., G. J. Massoth, R. A. Feely, R. W. Embley, R. E. Thomson, and B. J. Burd, Hydrothermal event plumes from the CoAxial seafloor eruption site, Juan de Fuca Ridge, *Geophys. Res. Lett.*, *22*, 147–150, 1995.

Baker, E. T., G. J. Massoth, R. A. Feely, G. A. Cannon, and R. E. Thomson, The rise and fall of the CoAxial hydrothermal site, 1993–1996, *J. Geophys. Res.*, this issue.

Ballard, R. D., R. Hekinian, and J. Francheteau, Geological setting of hydrothermal activity at 12°50′N on the East Pacific Rise: a submersible study, *Earth Planet. Sci. Lett.*, *69*, 176–186, 1984.

Bates, R. L., and J. A. Jackson, *Dictionary of Geological Terms*, 571 pp., Doubleday, New York, 1984.

Björnsson, A., Dynamics of crustal rifting in NE Iceland, *J. Geophys. Res.*, *90*, 10,151–10,162, 1985.

Björnsson, A., G. Johnsen, S. Sigurdsson, G. Thorbergsson, and E. Tryggvason, Rifting of the plate boundary in north Iceland, 1975–1978, *J. Geophys. Res.*, *84*, 3029–3038, 1979.

Brandsdottir, B., and P. Einarsson, Seismic activity associated with the September 1977 deflation of the Krafla central volcano in northeastern Iceland, *J. Volcanol. Geotherm. Res.*, *6*, 197–212, 1979.

Butterfield, D. A., I. R. Jonasson, G. J. Massoth, R. A. Feely, K. K. Roe, R. W. Embley, J. F. Holden, R. E. McDuff, M. D. Lilley, and J. D. Delaney, Seafloor eruptions and evolution of hydrothermal fluid chemistry, *Philos. Trans. R. Soc. London, Ser. A*, *355*, 369–386, 1997.

Chadwick, W. W., Jr., and R. W. Embley, Lava flows from a mid-1980s submarine eruption on the Cleft Segment, Juan de Fuca Ridge, *J. Geophys. Res.*, *99*, 4761–4776, 1994.

Chadwick, W. W., Jr., and R. W. Embley, Relationships between hydrothermal vents, intrusions, and ridge structure: High resolution bathymetric surveys using Mesotech sonar, Juan de Fuca Ridge, *Eos Trans. AGU*, *76* (46), Fall Meet. Suppl., F410, 1995.

Chadwick, W. W., Jr., R. W. Embley, and C. G. Fox, Evidence for volcanic eruption on the southern Juan de Fuca Ridge between 1981 and 1987, *Nature*, *350*, 416–418, 1991.

Chadwick, W. W., Jr., R. W. Embley, and C. G. Fox, SeaBeam depth changes associated with recent lava flows, CoAxial segment, Juan de Fuca Ridge: Evidence for multiple eruptions between 1981 and 1993, *Geophys. Res. Lett.*, *22*, 167–170, 1995.

Chadwick, W. W., Jr., R. W. Embley, and P. D. Johnson, Comparative study of recent eruptive sites on the Gorda and Juan de Fuca Ridges using AMS-60 sidescan sonar, *Eos Trans. AGU*, *77*(46), Fall Meet. Suppl., F1, 1996.

Cherkaoui, A. S. M., W. S. D. Wilcock, and E. T. Baker, Thermal fluxes associated with the 1993 diking event on the CoAxial segment, Juan de Fuca Ridge: A model for the convective cooling of the dike, *J. Geophys. Res.*, *102*, 24,887–24,902, 1997.

Choukroune, P., J. Francheteau, and R. Hekinian, Tectonics of the East Pacific Rise near 12°50′N: A submersible study, *Earth Planet. Sci. Lett.*, *68*, 115–127, 1984.

Curewitz, D., and J. A. Karson, Geological consequences of dike intrusion at mid-ocean ridge spreading centers, in *Faulting and Magmatism at Mid-Ocean Ridges*, *Geophys. Monogr. Ser.*, edited by W. R. Buck et al., AGU, Washington, D.C., in press, 1997.

Davis, P. M., The median valley, a result of magma fracture beneath mid-ocean ridges, *Nature*, *308*, 53–55, 1984.

Dziak, R. P., C. G. Fox, and A. E. Schreiner, The June–July 1993 seismo-acoustic event at CoAxial segment, Juan de Fuca Ridge: Evidence for a lateral dike injection, *Geophys. Res. Lett.*, *22*, 135–138, 1995.

Einarsson, P., Earthquakes and present-day tectonism in Iceland, *Tectonophysics*, *189*, 261–279, 1991.

Embley, R. W., and W. W. Chadwick Jr., Volcanic and hydrothermal processes associated with a recent phase of seafloor spreading at the northern Cleft segment: Juan de Fuca Ridge, *J. Geophys. Res.*, *99*, 4741–4760, 1994.

Embley, R. W., W. W. Chadwick Jr., M. R. Perfit, and E. T. Baker, Geology of the northern Cleft segment, Juan de Fuca Ridge: Recent lava flows, sea-floor spreading, and the formation of megaplumes, *Geology*, *19*, 771–775, 1991.

Embley, R. W., et al., Comparison of two recent eruptive sites on the Juan de Fuca Ridge: Geologic setting and time-series observations, *Eos Trans. AGU*, *75*(44), Fall Meet. Suppl., 617, 1994.

Embley, R. W., W. W. Chadwick Jr., and J. Getsiv, The CoAxial segment: A site of recent seafloor eruptions on the Juan de Fuca

Ridge, *Eos Trans. AGU, 76*(46), Fall Meet. Suppl., F410, 1995a.

Embley, R. W., W. W. Chadwick Jr., I. R. Jonasson, D. A. Butterfield, and E. T. Baker, Initial results of the rapid response to the 1993 CoAxial event: Relationships between hydrothermal and volcanic processes, *Geophys. Res. Lett., 22*, 143–146, 1995b.

Fornari, D. J., R. M. Haymon, M. H. Edwards, and K. C. Macdonald, Volcanic and tectonic characteristics of the East Pacific Rise crest 9°09′N to 9°54′N: Implications for fine-scale segmentation of the plate boundary, *Eos Trans. AGU, 71*(17), 625, 1990.

Fornari, D. J., R. M. Haymon, M. R. Perfit, T. K. P. Gregg, and M. H. Edwards, Axial summit trough of the East Pacific Rise 9°N to 10°N: Geological characteristics and evolution of the axial zone on fast-spreading mid-ocean ridges, *J. Geophys. Res.*, this issue.

Fox, C. G., W. W. Chadwick Jr., and R. W. Embley, Detection of changes in ridge-crest morphology using repeated multibeam sonar surveys, *J. Geophys. Res., 97*, 11,149–11,162, 1992.

Fox, C. G., W. E. Radford, R. P. Dziak, T. K. Lau, H. Matsumoto, and A. E. Schreiner, Acoustic detection of a seafloor spreading episode on the Juan de Fuca Ridge using military hydrophone arrays, *Geophys. Res. Lett., 22*, 131–134, 1995.

Gente, P., J. M. Auzende, V. Renard, Y. Fouquet, and D. Bideau, Detailed geological mapping by submersible of the East Pacific Rise axial graben near 13°N, *Earth Planet. Sci. Lett., 78*, 224–236, 1986.

Hauksson, E., Episodic rifting and volcanism at Krafla in north Iceland: Growth of large ground fissures along the plate boundary, *J. Geophys. Res., 88*, 625–636, 1983.

Haymon, R., D. J. Fornari, M. Edwards, S. Carbotte, D. Wright, and K. C. Macdonald, Hydrothermal vent distribution along the East Pacific Rise crest (9°9′–54′N) and its relationship to magmatic and tectonic processes on fast-spreading mid-ocean ridges, *Earth Planet. Sci. Lett., 104*, 513–534, 1991.

Haymon, R. M., et al., Volcanic eruption of the mid-ocean ridge along the East Pacific Rise crest at 9°45′–52′N: Direct submersible observations of seafloor phenomena associated with an eruption event in April 1991, *Earth Planet. Sci. Lett., 119*, 85–101, 1993.

Head, J. W., L. Wilson, and D. K. Smith, Mid-ocean ridge eruptive vents: Evidence for dike widths, eruption rates, and evolution of eruptions from morphology and structure, *J. Geophys. Res., 101*, 28,265–28,280, 1996.

Hekinian, R., et al. , East Pacific Rise near 13°N: geology of new hydrothermal fields, *Science, 219*, 1321–1324, 1983.

Holcomb, R. T., and J. L. Morton, Dive report: *Alvin* dive 1456, September 17, 1984, vent 3 area, southern Juan de Fuca Rift, *U.S. Geol. Surv. Open File Rep., 86-560-C*, 1–65, 1986.

Holcomb, R. T., E. Kappel, and S. Ross, Dive report: *Alvin* dive 1461, September 28, 1984, Plume site, southern Juan de Fuca Rift, *U.S. Geol. Surv. Open File Rep., 86-560-H*, 1–101, 1987.

Holden, J. F., B. C. Crump, M. Summit, and J. A. Baross, Microbial blooms at the CoAxial segment, Juan de Fuca Ridge deep-sea hydrothermal vent site following a magma intrusion, *Eos Trans. AGU, 76*(43), Fall Meet. Suppl., F411, 1995.

Jackson, D. B., D. A. Swanson, R. Y. Koyanagi, and T. L. Wright, The August and October 1968 east rift eruptions of Kilauea volcano, Hawaii, *U.S. Geol. Surv. Prof. Pap., 890*, 33 pp., 1975.

Juniper, S. K., P. Martineu, J. Sarrazin, and Y. Gélinas, Microbial-mineral floc associated with nascent hydrothermal activity on CoAxial segment, Juan de Fuca Ridge, *Geophys. Res. Lett., 22*, 179–182, 1995.

Kappel, E. S., and W. R. Normark, Morphometric variability within the axial zone of the southern Juan de Fuca Ridge: Interpretation from SeaMARC II, SeaMARC I, and deep sea photography, *J. Geophys. Res., 92*, 11,291–11,302, 1987.

Karson, J. A., et al., Along-axis variations in seafloor spreading in the MARK area, *Nature, 328*, 681–685, 1987.

Kong, L. S., R. S. Detrick, P. J. Fox, L. A. Mayer, and W. B. F. Ryan, The morphology and tectonics of the MARK area from SeaBeam and Sea MARC I observations (Mid-Atlantic Ridge 23°N), *Mar. Geophys. Res., 10*, 59–90, 1988.

Lagabrielle, Y., M. H. Cormier, V. Ballu, and J. M. Auzende, From perfect dome to large collapse caldera: Tectonic/magmatic evolution of the EPR axial domain at 17°–19°S from submersible observations, *Eos Trans. AGU, 77*(46), Fall Meet. Suppl., F660, 1996.

Larsen, G., K. Grönvold, and S. Thorarinsson, Volcanic eruption through a geothermal borehole at Namafjall, Iceland, *Nature, 278*, 707–710, 1979.

Lonsdale, P., Structural geomorphology of a fast-spreading rise crest: The East Pacific Rise near 3°25′S, *Mar. Geophys. Res., 3*, 251–293, 1977.

Macdonald, K. C., and P. J. Fox, The axial summit graben and cross-sectional shape of the East Pacific Rise as indicators of axial magma chambers and recent volcanic eruptions, *Earth Planet. Sci. Lett., 88*, 119–131, 1988.

Mastin, L. G., and D. D. Pollard, Surface deformation and shallow dike intrusion processes at Inyo Craters, Long Valley, California, *J. Geophys. Res., 93*, 13,221–13,235, 1988.

McConachy, T. F., R. D. Ballard, M. J. Mottl, and R. P. von Herzen, Geologic form and setting of a hydrothermal vent field at 10°56′N, East Pacific Rise: A detailed study using *Angus* and *Alvin*, *Geology, 14*, 295–298, 1986.

Moore, R. B., R. T. Helz, D. Dzurisin, G. P. Eaton, R. Y. Koyanagi, P. W. Lipman, J. P. Lockwood, and G. S. Puniwai, The 1977 eruption of Kilauea volcano, Hawaii, *J. Volcanol. Geotherm. Res., 7*, 189–210, 1980.

Murray, J. B., and A. D. Pullen, Three-dimensional model of the feeder conduit of the 1983 eruption of Mt. Etna volcano, from ground deformation measurements, *Bull. Volcanol., 47*(4), 1145–1163, 1984.

Mutter, J. C., G. A. Barth, P. Buhl, R. S. Detrick, J. A. Orcutt, and A. J. Harding, Magma distribution across ridge-axis discontinuities on the East Pacific Rise from multichannel seismic images, *Nature, 336*, 156–158, 1988.

Normark, W. R., J. L. Morton, R. A. Koski, D. A. Clague, and J. R. Delaney, Active hydrothermal vents and sulfide deposits on the southern Juan de Fuca Ridge, *Geology, 11*, 158–163, 1983.

Normark, W. R., et al., Submarine fissure eruptions and hydrothermal vents on the southern Juan de Fuca Ridge: Preliminary observations from the submersible *Alvin*, *Geology, 14*, 823–827, 1986.

Normark, W. R., J. L. Morton, and S. L. Ross, Submersible observations along the southern Juan de Fuca Ridge: 1984 *Alvin* program, *J. Geophys. Res., 92*, 11,283–11,290, 1987.

Opheim, J. A., and A. Gudmundsson, Formation and geometry of fractures, and related volcanism, of the Krafla fissure swarm, northeast Iceland, *Geol. Soc. Am. Bull., 101*, 1608–1622, 1989.

Pallister, J. S., Structure of the sheeted dike complex of the Samail Ophiolite near Ibra, Oman, *J. Geophys. Res., 86*, 2662–2672, 1981.

Park, R. G., *Foundations of Structural Geology*, 135 pp., Blackie & Son Limited, New York, 1983.

Parsons, T., and G. A. Thompson, The role of magma overpressure in suppressing earthquakes and topography: Worldwide examples, *Science, 253*, 1399–1402, 1991.

Perfit, M. R., and W. W. Chadwick Jr., Magmatism at mid-ocean ridges: Constraints from volcanological and geochemical investigations, in *Faulting and Magmatism at Mid-Ocean Ridges*, *Geophys. Monogr. Ser.*, edited by W. R. Buck et al., AGU, Washington, D.C., in press, 1997.

Phipps Morgan, J., and Y. J. Chen, Dependence of ridge-axis morphology on magma supply and spreading rate, *Nature, 364*, 706–708, 1993a.

Phipps Morgan, J., and Y. J. Chen, The genesis of oceanic crust: Magma injection, hydrothermal circulation, and crustal flow, *J. Geophys. Res.*, *98*, 6283–6297, 1993b.

Pollard, D. D., P. T. Delaney, P. T. Duffield, E. T. Endo, and A. T. Okamura, Surface deformation in volcanic rift zones, *Tectonophysics*, *94*, 541–584, 1983.

Renard, V., R. Hekinian, J. Francheteau, R. D. Ballard, and H. Backer, Submersible observations at the axis of the ultra-fast spreading East Pacific Rise (17°30′ to 21°30′S), *Earth Planet. Sci. Lett.*, *75*, 339–353, 1985.

Richter, D. H., W. U. Ault, J. P. Eaton, and J. G. Moore, The 1961 eruption of Kilauea volcano, Hawaii, *U. S. Geol. Surv. Prof. Pap., 474-D*, 34 pp., 1964.

Richter, D. H., J. P. Eaton, K. J. Murata, W. U. Ault, and H. L. Krivoy, Chronological narrative of the 1959–1960 eruption of Kilauea volcano, Hawaii, *U. S. Geol. Surv. Prof. Pap., 537-E*, 73 pp., 1970.

Rubin, A. M., Dike propagation and crustal deformation in volcanic rift zones, Ph.D. thesis, 205 pp., Stanford Univ., Stanford, Calif., 1988.

Rubin, A. M., Dike-induced faulting and graben subsidence in volcanic rift zones, *J. Geophys. Res.*, *97*, 1839–1858, 1992.

Rubin, A. M., and D. D. Pollard, Dike-induced faulting in rift zones of Iceland and Afar, *Geology*, *16*, 413–417, 1988.

Ruegg, J. C., J. C. Lepine, A. Tarantola, and M. Kasser, Geodetic measurements of rifting associated with a seismo-volcanic crisis in Afar, *Geophys. Res. Lett.*, *6*, 817–820, 1979.

Ryan, M. P., Neutral buoyancy and the structure of mid-ocean ridge magma reservoirs, *J. Geophys. Res.*, *98*, 22,321–22,338, 1993.

Ryan, M. P., J. Y. K. Blevins, A. T. Okamura, and R. Y. Koyanagi, Magma reservoir subsidence mechanics: Theoretical summary and application to Kilauea volcano, Hawaii, *J. Geophys. Res.*, *88*, 4147–4181, 1983.

Sigurdsson, O., Surface deformation of the Krafla fissure swarm in two rifting events, *J. Geophys.*, *47*, 154–159, 1980.

Sinton, J. M., and R. S. Detrick, Mid-ocean ridge magma chambers, *J. Geophys. Res.*, *97*, 197–216, 1992.

Smith, D. K., and J. R. Cann, Building the crust at the Mid-Atlantic Ridge, *Nature*, *365*, 707–715, 1993.

Spiess, F. N., and J. A. Hildebrand, Deep tow studies of recent activity on the Juan de Fuca Ridge, *Eos Trans. AGU*, *74*(43), Fall Meet. Suppl., 620, 1993.

Stein, R. S., P. Briole, J. C. Ruegg, P. Tapponnier, and F. Gasse, Contemporary, Holocene, and Quaternary deformation of the Asal Rift, Djibouti: Implications for the mechanics of slow spreading ridges, *J. Geophys. Res.*, *96*, 21,789–21,806, 1991.

Tarantola, A., J. C. Ruegg, and J. C. Lepine, Geodetic evidence for rifting in Afar: A brittle-elastic model of the behaviour of the lithosphere, *Earth Planet. Sci. Lett.*, *45*, 435–444, 1979.

Thorarinsson, S., The Lakigigar eruption of 1783, *Bull. Volcanol.*, *33*, 910–927, 1969.

Tunnicliffe, V., R. W. Embley, J. F. Holden, D. A. Butterfield, G. J. Massoth, and S. K. Juniper, Biological colonization of new hydrothermal vents following an eruption on Juan de Fuca Ridge, *Deep Sea Res.*, *44*, 1627–1644, 1997.

Wilcock, W. S. D., and J. R. Delaney, Mid-ocean ridge sulfide deposits: Evidence for heat extraction from magma chambers or cracking fronts?, *Earth Planet. Sci. Lett.*, *145*, 49–64, 1996.

Wilson, L., and J. W. Head, Nature of local magma storage zones and geometry of conduit systems below basaltic eruption sites: Pu'u 'O'o, Kilauea East Rift, Hawaii, example, *J. Geophys. Res.*, *93*, 14,785–14,792, 1988.

Wolfe, E. W., C. A. Neal, N. G. Banks, and T. J. Duggan, Geologic observations and chronology of eruptive events, in *The Pu'u 'O'o eruption of Kilauea volcano, Hawaii: Episodes 1 through 20, January 3, 1983, through June 8, 1984*, edited by E. W. Wolfe, *U. S. Geol. Surv. Prof. Pap., 1463*, 1–98, 1988.

W. W. Chadwick, Jr. and R. W. Embley, Hatfield Marine Science Center, Oregon State University, 2115 SE OSU Drive, Newport, OR 97365-5258. (e-mail: chadwick@pmel.noaa.gov)

(Received March 19, 1997; revised July 9, 1997;
accepted September 2, 1997.)